Investigation of Consumer Grade EEG as a Fall Risk Assessment Tool

by

Kaela Shea

A thesis

presented to the University of Waterloo

in fulfillment of the

thesis requirement for the degree of

Masters of Applied Science

in

Mechanical and Mechatronics Engineering

Waterloo, Ontario, Canada, 2017

Author's Declaration

I hereby declare that I am the sole author of this thesis. This is a true copy of the thesis, including any required final revisions, as accepted by my examiners.

I understand that my thesis may be made electronically available to the public

Abstract

Fall prevention for geriatric populations is a growing concern among clinicians and researchers due to severe risk of morbidity and loss of independence. Emerging evidence has demonstrated that cognitive workload while walking influences gait stability and the risk for falling. Electroencephalography (EEG) presents a potential method to provide objective measures, via Theta (4-7 Hz) and Alpha (8-13 Hz) frequency band powers, of cognitive workload during daily activities. Consumer grade EEG headsets increase the accessibility of EEG signal measurement through lowered cost and easier setup protocols. The following thesis presents a series of studies investigating the sensitivity of the Interaxon Muse headband, and the Emotiv Epoc+ to measure cognitive load changes under ambulatory conditions (i.e., while walking). While the Muse yielded no sensitivity to changes in neural activity associated with changes in cognitive load levels, the Emotiv Epoc+ yielded high sensitivity to cognitive load changes across all 14 electrodes. Further research concerning this thesis centred around the use of the Emotiv Epoc+ system to distinguish levels of cognitive load under ambulatory conditions.

To examine the impact of motion artifact on EEG signals measured by the Emotiv Epoc+, a swim cap paradigm was used to isolate noise associated with gait. Signal to noise ratio (SNR) estimates indicate that EEG signals are 8 to 20 times the power of gait-induced noise, supporting the Emotiv Epoc+ during ambulatory monitoring conditions. Applying time and spectral system identification techniques, the relationship between motion-induced artifacts and recorded inertial measurement unit (IMU) yielded a strong nonlinear response. The final study of this thesis evaluated the utility of the Emotiv Epoc+ to measure 3 levels of cognitive load using a working memory paradigm while walking on a treadmill. A quadratic support vector

machine (SVM) classifier was able to classify three levels of cognitive load at an accuracy of 70.3 %. These promising initial results, coupled with the short measurement time (10 sec), support the long-term goal of assessing cognitive load in an ambulatory environment towards implementation in fall risk assessment systems.

Acknowledgements

Research presented in the following thesis is supported by the National Sciences and Engineering Research Council of Canada (NSERC).

I would like to thank the research group at the Toby Jenkins Applied Health Research Building, Dr. Laura Middleton, and Spencer Wikkerink of the Department of Kinesiology for their knowledge and patient assistance.

A special thanks to my supervisor Dr. James Tung for his support throughout this research.

Table of Contents

List of Figures

List of Tables

Chapter 1

Introduction

Numerous studies have demonstrated an interdependence between gait instability and cognitive impairment in older adults and are gaining acceptance as a factor in fall risk assessment [2]. While methods to quantify gait stability are available (i.e., gait analysis tools), complementary capabilities to measure cognitive load remain to be developed. To address the need for more sensitive metrics of cognitive load to assess fall risk, electroencephalography (EEG) presents a potential method [3]. While traditional EEG systems are resource-intensive and require long setup times, recent commercialization of EEG systems have provided a promising alternative to acquire EEG signals ([4], [5]). Despite the potential of commercial EEG technology for attaining a new perspective on cognitive workload recording, constraining factors limit the use of EEG systems outside of a research lab. In particular, motion artifacts have been identified as major barriers in the acquisition of sufficiently high quality signals [6].

1.1 Scope

By directly measuring cognitive load in daily life, individuals may be assessed for activities that contribute to high cognitive load levels, a factor related to the risk of falling. This detailed information may be used to identify individual risks (e.g., walking while talking or 'texting'). The following thesis addresses the possi-

bility to leverage accessibility, in mobility and cost, of commercially available EEG systems for measuring cognitive load during daily routines as part of a wearable fall risk assessment system. Studies presented in the following thesis are designed to investigate the capacity of a consumer grade EEG system to measure cognitive load during ambulatory activities and explore signal processing techniques to mitigate challenges with artifact-corrupted EEG data.

1.2 Outline

This thesis begins with Chapter 2, reviewing the scientific literature related to dual-tasking and falls, cognitive load, and EEG research related to this thesis. In Chapter 3, an exploratory investigation of the performance of two commercially available systems, the Muse [7] and Emotiv Epoc+ [4], was conducted. The initial evaluation determined whether data acquired from the Muse was sensitive to varying levels of cognitive load during an ambulatory measurement procedure. Subsequently, the Emotiv Epoc+ system was compared with a 'gold standard' cap (Compumedics SynAmps 2/RT Quik-Cap Ag/AgCl 64 channel cap). While the wireless and dry-electrode systems were quick and easy to set up relative to the research-grade system, motion artifact was a concern. These exploratory studies found data obtained from the Muse during walking was overpowered by motion artifact, while the Emotiv demonstrated more promising results indicating sensitivity to cognitive load levels. In Chapter 4, further investigation into the noise corruption of the EEG data measured by the Emotiv related with motion artifact was performed, including estimates of signal-to-noise ratio (SNR), and noise modelling using system identification techniques. Based on strong SNR estimates, Chapter 5 describes a study to examine whether the Emotiv Epoc+ distinguished varying levels of cognitive challenge in a working memory task while treadmill walking. Each experimental investigation is presented, analyzed, and discussed in the following chapters. Research findings and insights are concluded in the final chapter, Chapter 6.

Chapter 2

Literature Review

Falls are considered a major problem in the older adult population. An assessment of age association of fall related mortality, adjusting for comorbidities, found the mortality of a fall related hip fracture increases with age [8]. In addition to increased risk of death, falls are the cause of severe trauma, are implicated in multiple comorbidities, and are a burden on health care resources and the community. Based on fall incidence studies, 2.2 % of hospitalizations in a year in the United States of America are caused by a ground level fall, 12.2 % of which require intensive care unit stays, and 4.8% will result in death [9]. After release from a hospital only 16 % of older adults who lived independently before their fall will return to independent living. It is estimated that 30% of individuals aged 65 years and older experience at least one fall each year, a rate which increases with age [10]. Additionally, individuals with previous history of falls are at a higher risk of future falls [11]. Canada has an aging population with growing number of older adults to care for and falls contribute to a large proportion of the population needing care.

Clinical evidence demonstrates that fall prevention programs are moderately effective. There are many strategies for fall prevention including: education, modification of the home environment, and physical training [12]. Interventions that use individualized multifactorial assessments to target key risk(s) have proven to be the most effective within community based fall prevention programs ([13], [14], [15]). A

review of the literature yielded 60 randomized control trials supporting the effectiveness of multifactorial fall prevention programs [14], as well as cost-benefit economic analyses [16]. Despite encouraging research and awareness of the risk and severity associated with falling [17], there exist limited clinical efforts at preventing falls in an older adult population [14]. A systematic review of fall prevention strategies to identify barriers and facilitators involved with fall prevention in residential care found social and organizational layers of the programs were most influenced. Facilitators for older persons' involvement in fall prevention programs included communication and facility equipment availability, while barriers included frustration and limitation in knowledge among the staff [18]. Technology has the potential to reduce the workload and dependency fall prevention programs place on staff through automated continual monitoring, however a review of sensor systems implemented for fall prevention yielded inconsistent results [19]. One identified barrier to technology transfer of fall prevention technologies is a limited range and scope of metrics.

An emerging factor in falls research has examined the influence of cognitive capabilities on gait instability and risk for future falls. Aging is associated with multi-sensory inhibition in addition to neurophysiological degeneration. Even a healthy aging process will result in loss of motor neurons, decreased nerve conduction, limited proprioception, muscle weakness, and reduced cognitive processing abilities [20]. Horak [21] found that, due to a decline in cognitive processing abilities, older individuals lack the ability to quickly re-weigh sensory information and adapt to environmental change. A lack of ability to efficiently and effectively adapt to environmental changes may be a contributing factor in gait instability among a geriatric population. There have, however, been differences between gait of younger and older adults noted in studies performed on a level, invariable, surface [20] [22]. This observation indicates there are further factors that influence gait stability in seemingly healthy older adults.

In healthy young adults, muscle activity is controlled automatically through motor pathways, primarily with the cerebellum and basal ganglia; producing periodic spatio-temporal patters in gait [23]. Voluntarily induced motion is controlled by centres in the primary motor cortex, premotor cortex in the frontal lobe

and parietal lobe, as well as the corticobulbar and corticospinal pathways [23]. With neurological decline associated with age, motor tasks necessary for gait are more reliant on voluntary control and become cognitively taxing [24]. Consistent spatiotemporal gait parameters reflect that there exists little input from higher cortical regions, while variability indicates high amounts of voluntary control over gait. In analyzing neurophysiological control of gait, Hausdorff et al. [20] discovered a marked distinction between spatiotemporal fluctuations in gait of young adult subjects and older subjects. Older subjects exhibited more random fluctuation of stride in comparison with the control group [20]. More high cortical interaction in the control of gait has been shown to indicate decline in cognitive processes such as attention, working memory, and executive function that are associated with early stages in dementia.

As older individuals depend more on cognition for the control of gait relative to the automatic process in healthy younger adults, more focus is required. A dual task paradigm involves the subject performing two tasks that demand the subject's attention, competing for their cognitive resources. Gait, as a complex procedure requiring attention, executive function, and working memory, demands a significant cognitive load [25]. It has been shown that at an increased load of cognitive activity, the subjects tend to exhibit modifications to their gait, such as slowing, as a compensatory action. The higher the cognitive load that the subject experiences while performing a dual task paradigm while walking, the more the subject is at risk of a fall [2].

Mounting evidence drawn from dual-task paradigms, where individuals walk while performing a secondary cognitive task, demonstrate a robust relationship between cognitive load and gait instability. As older individuals must dedicate more cognitive resources to the action of maintaining a stable gait, additional tasks negatively impact gait performance and stability ([25], [24], [26]). For example, Iersel et al. [27] demonstrated a relationship between performance on working memory tasks and reduced gait stability. Doi et al. [22] found a strong association between mild cognitive impairment and an increased rate of falling. When focusing on older individuals with mild to sever cognitive impairment, Montero-Odasso et al. [2] found the rate of population that experience at least one fall event per year to be more than double that of

the older population in general at 60% to 80% per year. As a result, there is increasing interest in translating these findings to advance fall risk assessment tools.

The overarching goal of this thesis is to advance fall risk assessment tools by developing new indices of cognitive load under dual-tasking conditions (i.e., walking while performing a secondary task). While previous research examining dual-task effects have focused on sensitive gait performance metrics (e.g., step time variability), complementary methods to measure cognitive load are few. Physiological measures that are strongly supported in literature to provide information on cognitive load include: heart-rate variability, brain activity, and hormonal (e.g., Adrenaline, Noradrenaline) levels. However, heart rate variability and hormone level changes are not uniquely dependant on levels of cognitive load. Additionally, these physiological measures are insensitive to instantaneous cognitive load changes in the case of heart rate variability, and have a long rise time, in the case of hormone level changes [28].

Methods to measure brain activity remain strong candidates to measure changes in cognitive load [28]. Brain imaging studies have provided target areas for consideration, particularly lateral prefrontal areas. Functional Magnetic Resonance Imagining (fMRI) research demonstrates that an increased cognitive load through performing a working memory task, compared to a resting state, increases activity in the dorsolateral prefrontal cortex. Working memory tasks have also exhibited increased functional connectivity between the inferior parietal cortex and dorsolateral prefrontal cortex [29]. Additional regions associated with cognitive load were predicted through Transcranial Magnetic Stimulation (TMS) studies. For example, the visual cortex (i.e., occipital lobe) was found to participate in storing precise visual working memory information. The lateral prefrontal cortex region has been found to remain active throughout maintenance of the working memory, processing and integrating information related to multiple stimuli including sensorimotor, parietal, and visual regions [30]. However, imaging techniques are limited due to temporal delays associated with hemodynamic response, and the expense and limited mobility of the equipment [31].

Electroencephalogram (EEG) presents a unique brain activity measurement modality that is less restric-

tive to participants relative to brain imaging modalities (i.e. fMRI, functional Near-Infrared Spectroscopy (FNIRS), and positron emission tomography (PET)) and has the capacity to capture instantaneous fluctuations in cognitive load [32]. Briefly, EEG measures electrical activity associated with neurocognitive function through electrodes applied to the scalp to capture a summation of post synaptic potentials across a broad neural area [33]. In comparison to fMRI and PET imaging techniques, this neuro-physiological technique allows for movement of the participant, as the subject is restricted only by light weight electrodes and miniaturized amplifiers. Considering the goal of acquiring cognitive load under ambient conditions, there exists an importance in measuring cognitive load during motion, as opposed to cognitive tasks being presented to a stationary participant [34]. The high temporal resolution of the EEG allows immediate neurological reactions to stimuli to be recorded.

Based on existing literature, oscillatory frequency of the EEG signal can provide insight into the functional networks of the cortex as a defined range of frequencies are correlated with specific brain activities [32]. Five distinct frequency bands have been identified in the human brain: Delta, Theta, Alpha, Beta, and Gamma. The two spectra relevant for measurement of cognitive load are Theta (4-7 Hz) and Alpha (8- 13 Hz) bands [33], including established correlations to information processing tasks [32]. Studies measuring Alpha and Theta waves using EEG technology demonstrate decreases in band powers during increasingly challenging working memory tasks, with strong reliability in measuring cognitive load ([35], [33], [36], [37]). Fundamental neuro-anatomical sources of Theta and Alpha frequencies continue to be investigated, however the weight of current evidence indicates changes Theta and Alpha frequency powers are correlated to cognitive load. A summary of EEG sites that correspond to the regions of interested for changes in cognitive load are shown in Table 2.1 and are depicted visually in Figure 2.1.

Table 2.1: Summary of cortex regions with activity associated with cognitive load and their corresponding EEG sites

Anatomical Region	**EEG 10-10 measurement site**
Lateral prefrontal cortex	F4, F3, F2, F1, FZ , AF4, AF3, AF2
Inferiorparietal cortex	CP3, CP4, CP5, CP6, P3, P4, P5, P6
Visual cortex	O1, O2, OZ

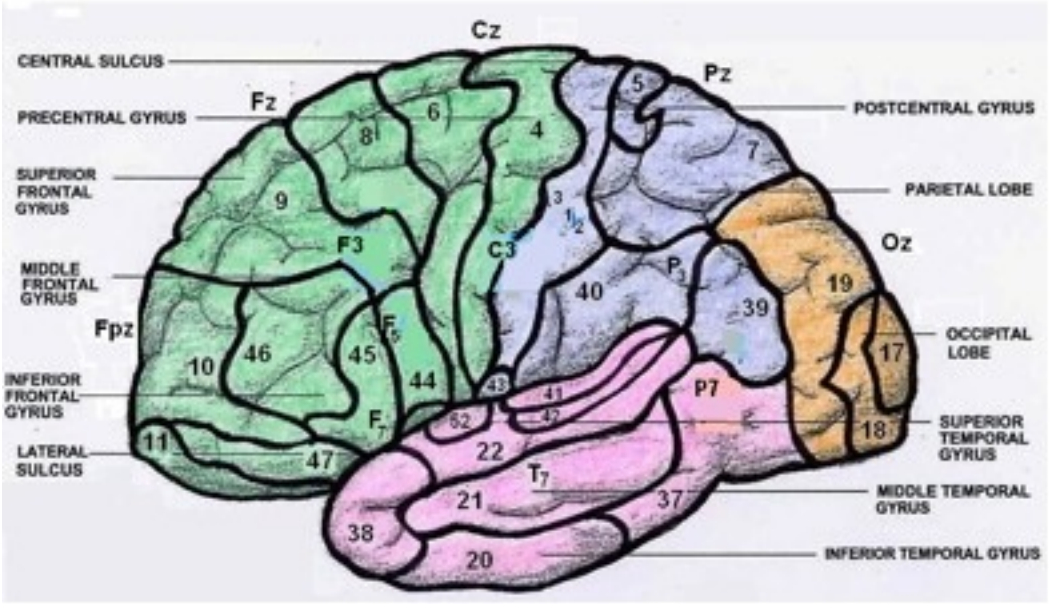

Figure 2.1: A comparison of the electrode positions according to the international 10/20 system, internationally recognized EEG electrode placement locations and labels, relative to functional regions of the brain. Numbers correspond to specific functional regions of the brain that are briefly described by the text labels. Alphanumeric labels correspond to EEG international 10/20 electrode sites. Colours reference major anatomical lobes of the brain; green corresponds to the frontal lobe, blue corresponds to the parietal lobe, pink corresponds to the temporal lobe, and orange corresponds to the occipital lobe. [1]

Commercialized EEG systems offer a more financially accessible and "easy to use" option for attaining EEG signals as compared to research grade EEG systems [38]. Two consumer grade EEG measurement systems investigated in this thesis are the Muse ([7]) and the Emotiv Epoc+ shown in Figure 2.2b ([4]). The Muse, developed by Interaxon, captures EEG signals through four dry bio-potential electrodes (TP9, AF7, AF8, TP10) with a reference electrode at FPZ, a three axis accelerometer, and is capable of measuring frequencies of the Delta, Theta, Alpha, and Beta bands [5].

(a) Image of Interaxon's Muse [7]

(b) Picture taken of the Emotiv Epoc +

Figure 2.2: Devices, Muse and Epoc+, used in the study

The Emotiv Epoc+, produced by Emotiv Inc, is a wireless headset measuring EEG signals at 14 different electrode sites; AF3, F7, F3, FC5, T7, P7, O1, O2, P8, T8, FC6, F4, F8, AF42. The Emotiv Epoc+ is more prevalent in literature. Although suitability of the Emotiv Epoc+ is dependant on the research paradigm, many evaluations have found the Emotiv Epoc+'s performance to be satisfactory for non-clinical applications ([39], [38]). The Emotiv Epoc+ EEG measurement system records tri-axial acceleration with an inertial measurement unit (IMU) built into the device [4]. A key feature the Emotiv Epoc+ is the use of saline electrodes mounted to an adjustable headset, significantly reducing time required to prepare as it avoids use of the gel electrodes used in traditional EEG systems [4]. Lin et al. [40] successfully measured steady state evoke potentials using the Emotiv Epoc+ system during treadmill walking that mimics day-to-day gait. Furthermore, Duvinage et al. [41] evaluated the intrinsic performance of the Emotiv Epoc+ system relative to a research grade ANT Waveguard system. While the researchers concluded that Emotiv Epoc+ performance proved acceptable, the study found that the medical grade system did significantly outperform the Emotiv Epoc+ during motion [41]. A summary table of Emotiv Epoc+ and Muse technical specifications can be found below (see Table 2.2).

Table 2.2: Summary of technical specifications of the Muse and Emotiv Epoc+ EEG capture systems

Technical Specifications	Emotiv Epoc+ System	Muse System
IMU Signals	3D accelerometer, 3D gyroscope, 3D magnetometer	3D accelerometer
IMU Sampling Rate	64 Hz	50 Hz
Number EEG of Electrodes	14	4
EEG Sampling Rate	128 Hz	220–500 Hz
Data Transmission	Bluetooth	Bluetooth
Resolution	14 bit	10–16 bit
Signal Bandwidth	0.2–43 Hz	2.5–44 Hz
Built in Filters	5th order Sinc 50 Hz and 60 Hz notch	DRL – REF feedback 50 Hz and 60 Hz notch
Battery Life	12 hours	5 hours

The contamination of measured EEG signal with undesired signal artifacts produced due to movement is defined as motion artifact [42]. Motion artifacts in EEG are difficult to identify and obscure (desired) neural information. Many simple artifact removal techniques, such as signal subtraction and filtering, often result in the degradation of the quality of signals of interest [43]. Even powerful signal processing tools such as Blind Source Separation, including Independent Component Analysis (ICA), are associated with high computational expense and cannot reliably mitigate noise induced through full body motion ([44], [43]). An extensive review of methods for the detection and removal of artifacts from EEG revealed no universally accepted artifact detection or rejection technique. Identifying the characteristics of artifacts remains the most important step in mitigating their influence on signals. However, in absence of ground truth motion artifact data in literature, popular methods for removing EEG artifacts rely on estimating the influence of poorly characterized artifacts in data [43]. To develop sufficient understanding of the corrupting artifact, Oliveira et al [44] suggested the influence of motion on EEG must be recorded directly. During gait, head movement has demonstrated the strongest correlation in the vertical axis of motion ([45], [46]). Oliveira et al. [44] attempted to model motion artifact using a phantom head model on a robotic arm to induce vertical displacement. Examination of motion artifact from actual human motion, however, remains under-examined.

Using a novel human paradigm, Kline et al. [47] investigated motion artifacts introduced through gait. Physiological signal measurement was blocked using a silicone swim cap such that electrodes of the EEG cap recorded only motion artifact. Regression techniques were applied to create a linear model relating head movement and motion artifact [47]. The authors concluded walking speed and did not yield a strong linear relationship to head acceleration.

In summary, literature shows a need for efficient fall prevention tools. Designing new tools for fall risk assessment may provide the potential to improve independence and quality of life of older individuals, as well as reduce the social and economic costs of caring for those who have suffered an injury from falling. A relationship between cognition and gait shows that increased cognitive load may put older individuals at risk of falling [2] [25] [48] [49]. This research will provide insight for the optimization of a consumer grade neuroimaging system that may be employed in a wearable system to continuously monitor cognitive load. This analysis will provide an individualized assessment to identify activities that contribute to periods of high cognitive load.

Chapter 3

Exploration of Commercial EEG System Capabilities

There exists a benefit in measuring human cognition in it's natural form. Investigating active human cognition while an individuals interacts within a four dimensional environment with complex sensory experiences may provide a unique and valuable insight into the management of cognitive resources [34]. Cognitive decline, including age-related deterioration, reduces cognitive resources available for allocation. As gait stability depends on executive function, gait instability and cognitive impairment are interdependent, and are powerful indicators for a risk of falling. In a dual task paradigm, the brain may allocate cognitive resources to one task over the other (i.e., prioritizing the performance of one task). The influence of dual tasking has been exhibited as costs in gait performance, such as changing stride length and gait speed. In day-to-day life these gait performance costs caused by multiple task environments creates instability in gait [2].

This chapter presents an exploratory study that investigates the potential for the use of commercially available EEG systems in the place of research grade EEG systems for measuring cognitive load in dual motor and cognitive task paradigms. Relative to research grade EEG systems, consumer grade EEG systems increases accessibility of neural measurement through increased mobility and reduced cost. The following

chapter describes a study examining Interaxon's Muse and Emotiv's Epoc+ performance for measuring Alpha and Theta frequency band power differences associated with cognitive load paradigms during motion. Previous studies have found sufficient capacity of the Epoc+ for applications such as brain-computer interfaces, language processing, and P-300 component detection [38]. Grummett et al. [39] compared the performance of three consumer grade EEG systems (Emotiv Epoc+, B-Alter, g.Sahara) with a research grade system (g.HIamp) on metrics including the ability to measure Alpha activity, visual steady-state response, P300, and event related desynchronization and synchronization. With respect to the performance of the Epoc+, it was found that the Epoc+ lacked sufficient electrode positions for evant-based synchronization methods. However, the Epoc+ was able to measure Alpha activity with acceptable accuracy and sensitivity [39]. In comparison with the Neurosky and the MindWave, Maskeluinas at al. [50] found the Epoc+ to be more suitable for use with control tasks due to superior recognition in attention level and blinks.

Literature investigating the applications of the Muse measuring EEG signals is much less robust relative to the Emotiv. Athavale and Krishnan [5] explored wearable bio-signal monitoring citing the values of EEG signal monitoring extending from diagnosis of neuro diseases, to brain-computer interfaces, to stress assessment and mental health. The study performed no assessment into the accuracy of EEG signals measured by the Muse, however noted that the electrode number of the Muse (four) limits its use case [5]. The Interaxon's Muse has a more user centred design relative to the Emotiv Epoc+ system, providing more comfort and a lower profile device. Although the Muse design has a very minimal amount of electrodes, locations of the electrodes include the prefrontal and parietal cortices that are relevant in changes in cognitive load.

The investigation into the performance potential of consumer grade EEG systems was performed in two experiments. The first experiment focused on the capacity of the Muse to perform during ambulatory conditions, while the second experiment involved a comparative study between the Emotiv Epoc+ and a research grade EEG system. It was hypothesized that Interaxon's Muse and the Emotiv Epoc+ systems would be capable of measuring EEG signals at a sufficient quality to differentiate between cognitive load levels. All

subjects included in this study provided informed written consent; with approval from the Office of Research Ethics at the University of Waterloo.

3.1 Experiment 1: Muse

The Interaxon's Muse device was designed for paradigms involving minimal movement [7], such as meditation. Due to lack of supporting literature and the device's intended use case, the initial consideration for involving the Muse as a method of recording neural activity in ambulatory environments, was its capacity to reliably record EEG signals during gait. In Experiment 1, the Muse was evaluated to determine whether the device is capable of distinguishing varying levels of dual-tasking conditions. It is hypothesized that the Muse would be sensitive to established methods of eliciting increased cognitive load associated with dual-tasking conditions.

3.1.1 Methods

Experimental Setup

Nine individuals ages 18 to 25 with no neurological impairments or current physical impairments volunteered for participation in this phase of the study. All subjects provided informed written consent; the Office of Research Ethics at the University of Waterloo approved this study protocol. Interaxon's Muse headset was used to measure EEG signals throughout the trials. The Muse was used as directed (Refer to Appendix B.1), measuring signals from sites TP9, AF7, AF8 and TP10 [7]. Raw data transmitted from the Muse was recorded over the Bluetooth communication controlled through the computer's operating system command line.

Data Collection Tasks

Volunteers participated in six, two minute trials: three single task trials and three dual task trials. The single task trials consisted of a serial subtraction task during which participants repeatedly subtracted the same subtrahend from a given random starting number, and the difference of each operation being the next minuend. A random starting integer was chosen such that serial subtraction, in the allotted time, would not yield a negative difference. The subtrahends used in the three trials were 1, 3, and 7 to elicit increasing cognitive load levels. The task was chosen to exercise working memory, with capability to be performed during walking. Participants performed the serial subtraction tasks verbally while seated during single task trials, and while walking at a self-selected speed during dual task trials. Each session performed the trials in a random order. Participants were instructed prior to beginning the trial to continue the serial subtraction regardless of any suspected errors.

Data Processing and Analysis

Captured data was processed offline using MatLab (v2016a). Alpha frequency signals were segmented using a least squares finite impulse response (FIR) bandpass filter. A sliding 10 second Kaiser window with 5 seconds of overlap was used to segment the electrode signals into epochs. Each epoch was detrended using the mean calculated across every electrode channel and all time epochs. Frequency band power values were calculated per 10 second epoch by the square of the root mean square value (see Equation 3.1). A two-way analysis of variance (ANOVA) analysis was applied to each participant to determine the influence of two main effects: 1) level of cognitive challenge (i.e., subtraction by 1, 3, or 7), and 2) task condition: single (i.e., seated) or dual-tasking (i.e., walking), on Alpha frequency band power change. To maximize data power, all 10-second epochs from each of the four electrodes were considered samples. The null hypothesis of the ANOVA is that no significant change exists in Alpha frequency band powers between levels of cognitive challenge and the different task conditions. To asses whether the Muse device was capable of measuring

cognitive load associated with dual-tasking (i.e., motion) and increasing cognitive task difficulty (i.e., 1- vs 2-back), the ratio of participants exhibiting significant changes was examined.

$$Power = \sum_{i=1}^{M} \frac{|u_i|^2}{M} \tag{3.1}$$

where u_i represents the ith element in an array of M elements.

3.1.2 Results

The data analysis described above provided insight into the impact of different dual-task conditions on the EEG signal power in Alpha frequency bands. Two conditions analyzed through the ANOVA are cognitive load levels and motion (i.e., walking). If there exists a statistically significant difference in the data sets of different conditions, the ANOVA will produce a significant p value. Table 3.1 provides the p values attained through applying the ANOVA to the Alpha powers calculated from the EEG signal data obtained from the Muse. For the majority (5/9, 56%) of participants, motion significantly impacted the power of the Alpha frequency band, while the interaction between the two main effects yielded significant changes in power in 1 of 9 (11%) participants. No significance was seen the the varying cognitive load.

3.1.3 Discussion

The hypothesis that consumer grade Muse EEG systems would be sensitive to changes in cognitive load associated with task difficulty and motion was investigated in this experiment. Cognitive load was induced in different levels through a serial subtraction task performed while stationary for single task trials and while walking for dual task trials. Alpha frequency band powers were calculated from 10 second epochs of electroencephalography (EEG) signals were measured by the Muse during the six trials. An Analysis of Variance (ANOVA) was applied to the Alpha powers of the various levels of cognitive tasks during single and dual task trials to analyze the influence of motion and cognitive load on Alpha powers. It is important to

Table 3.1: Results of ANOVA on Alpha (8-13 Hz) power by participant and main effects, movement and cognitive load. Displayed are the p values where p$\leq$ 0.05 is considered significant and are marked with asterisks.

Participant	**Effect of motion**	**Effect of cognitive load**	**Interaction**
1	0.03*	0.54	0.53
2	0.00*	0.37	0.86
3	0.00*	0.59	0.39
4	0.35	0.21	0.07
5	0.56	0.49	0.00*
6	0.00*	0.94	0.68
7	0.21	0.49	0.93
8	0.94	0.58	0.73
9	0.05*	0.15	0.43

56% of participants yielded significant Alpha values due to motion, 0% due to cognitive load changes, 11% showed significant interaction between the two main effects.

note we did not verify distribution of Alpha frequency powers in the data used in the Analysis of Variance here. While it is assumed, verification of a normal data distribution should be performed to support the results of the ANOVA.

Results of the ANOVA found changes in cognitive load did not statistically significantly influence the power of Alpha signals in the EEG data measured by the Muse, as displayed in Table 3.1. Additionally the interaction between the two factors, motion and cognitive load, was shown to not produce any statistically significant changes in the power of Alpha frequency signals, with exception to one participant out of seven. The addition of motion was confirmed by the ANOVA to significantly influence the Alpha frequency band powers in 5 of 9 of the participant's data.

Drawing from prior literature, a significant decrease in Alpha band power was expected with increased cognitive load [33]. Given the results of the ANOVA it is likely that the Muse headset was overpowered by motion artifact during ambulatory conditions. The use case confirmed the Interaxon for the Muse is for use in meditation, a stationary practice, as such, it cannot be expected design features of the Muse to be optimal for ambulatory conditions. That the Muse is not designed for use during motion is evident from a loose fit of the Muse to the user that prioritized comfort and does little to fix the electrodes in place. Addition-

ally the dry electrodes, while convenient for consumer use, will also result in a high amount of electrode movement relative to wet electrodes. The Muse also has electrode placement restricted to the frontal and temporal lobes, Gerlic and Jausovec [37] however measured significant changes in Alpha frequency power in the parietal lobe. Considering the lack of effect associated with cognitive load and lack of interaction effect between the two considered factors, the hypothesis that the Muse is sensitive to changes in cognitive load is rejected.

3.2 Experiment 2: Emotiv Epoc+

The capability of the Emotiv Epoc+ system to provide sufficient quality of EEG signals in a variety of research scenarios is well supported. The aim of the second experiment of this study therefore was to ensure the quality of the Emotiv Epoc+'s captured EEG signals, in the particular paradigm of measuring cognitive load, is comparable to that of a research grade EEG system. It is hypothesized that the Epoc+ would be sensitive to increased cognitive load associated with dual-tasking conditions, comparable to a research-grade EEG system, the Compumedics SynAmps 2/RT Quik-Cap Ag/AgCl 64 channel cap. Some of the following information regarding Experiment 2 has been presented in brief at IEEE EMBS 2016 Conference as a one page paper.

3.2.1 Methods

Experimental Setup

Seven individuals ages 18 to 25 with no neurological impairments or current physical impairments participated in this experiment. Two EEG measurement devices were compared; the Emotiv Epoc+ system and a Compumedics SynAmps 2/RT Quik-Cap Ag/AgCl 64 channel cap. Sites of measurement corresponded to the overlap between the Compumedics electrode cap and those of the Emotiv Epoc+ system (F3, F4, C3,

C4, P3, and P4). Each device was set up according to their directed use (Refer to Appendix A.2 and A.3).

Data Collection Tasks

Participants underwent three, five minute trials. Two trials simulated dual task environments with a motor task being performed in conjunction with a working memory task of two levels of challenge, and a single task trial was performed with the easier version of the working memory tasks performed in isolation. The motor task involved riding a stationary bike at a self-selected leisurely pace and resistance. The cognitive tasks were continuous n-back memory tests, in which a series of random numbers was presented at 1 Hz on a monitor. In the easier version, participants compared the sequence of numbers to the number shown at the beginning of the trial. In the hard version, a 2-back test, participants compared the current number to one shown two previously in the sequence [51]. Participants were instructed to press a button when the number presented to them constituted a match. Participants performed tasks first with one EEG device, then repeated with the other. The order of trials were randomized between participants.

Data Processing and Analysis

EEG data was processed offline using MatLab (v2016a). Theta (4-7 Hz) and Alpha (8-13 Hz) frequency bands were segmented using a lease squares FIR bandpass filter. Similar to Experiment 1, a 10 second sliding Kaiser window was used to segment the electrode signal into epochs. Each epoch was detrended using the mean of data across every electrode channel and all time epochs. The frequency power values were calculated per 10 second epoch by the square of the root mean square value (see Equation 3.1). Single task powers were used as baseline for each participant to aid in the comparison of data from the Compumedics and Emotiv systems. The measure for low cognitive load was taken as the difference between the frequency powers of the dual task paradigm with easy cognitive task, and the frequency powers of the single task paradigm. Likewise, the measure for high cognitive load was taken as the difference between the frequency

powers of the dual task paradigm with the hard cognitive task, and the frequency powers of the single task paradigm. These calculations, illustrated in Equation 3.2, were taken for both the Emotiv and Compumedics systems. Alpha and Theta frequency band powers for low and high cognitive load paradigms were averaged across the electrodes per trial providing a value of Alpha and Theta frequency band power per participant for low and high cognitive load paradigms. To account for the possibility of large variances in signals measured at different neuro-anatomical regions, analysis of EEG data was also performed per electrode location. Alpha and Theta frequency band powers were averaged across the seven participants per electrode location for the location based analysis.

$$lowCognitiveLoad = dualEasyTask - singleEasyTask \tag{3.2}$$

$$highCognitiveLoad = dualHardTask - singleEasyTask \tag{3.3}$$

Paired t-tests were used to test for significant differences in frequency band powers between the two levels of cognitive load (i.e., low cognitive load, and high cognitive load as calculated in Equation 3.2) for each electrode channel location. Significance was defined as a p value equal or less than 0.05. To compare between measurement devices, the number of electrode sites indicating significantly different powers by cognitive load was calculated.

3.2.2 Analysis of Emotiv Epoc+–Compumedics Comparison

As shown in Tables 3.2 and 3.3, a participant based analysis of the EEG data, the Compumedics system was more sensitive in measuring differences in Alpha and Theta band power associated with changes in cognitive load for the majority of electrode locations. Data captured using the Compumedics system yielded 9 out of 12 significant power changes associated with dual-task conditions. In comparison, 5 of 12 observations were significantly different for the Emotiv Epoc+.

Table 3.2: Mean of the Alpha and Theta band power across 5 minute trials of Emotiv Epoc+ data for dual task trials and the single cognitive task trial. Values in parenthesis indicate the standard error. Significant data sets for a two sample t-test ($p<0.05$) are marked with asterisks(*).

Frequency	**Participant**	**Low Cognitive Load** Mean Power (SE)	**High Cognitive Load** Mean Power (SE)
Alpha	1	12.8 (1.3)	13.6 (2.0)
	2	20 (1.2)	14 (1.6)
	3*	838.6 (42.6)	$2.0x10^3$ (152.8)
	4	37.2 (7.8)	75.1 (33.4)
	5	29.6 (10.1)	14.3 (1.9)
	6*	$4.9x10^5$ ($8.7x10^3$)	$7.1x10^4$ ($2.8x10^3$)
	7	44.5 (2.6)	103.5 (5.9)
Theta	1	34.3 (4.4)	46.7 (11.6)
	2	74.5 (9.2)	81.9 (18.1)
	3*	$3.6x10^3$ (157.6)	$1.2x10^4$ (975.9)
	4	115.8 (15)	187.9 (87.8)
	5	152.8 (44.1)	59.4 (10.8)
	6*	$1.2x10^6$ ($2.6x10^4$)	$4.1x10^5$ ($1.7x10^4$)
	7*	208.4 (11.5)	609.3 (35.9)

Table 3.3: Mean of the Alpha and Theta band power across the 5 minute trials of Compumedics system data for dual task trials and the single cognitive task trial. Values in parenthesis indicate the standard error. Significant data sets for a two sample t-test ($p<0.05$) are marked with asterisks(*).

Frequency	**Participant**	**Low Cognitive Load** Mean Power (SE)	**High Cognitive Load** Mean Power (SE)
Alpha	1*	6.1^4 (3.3^3)	6.3^4 (3.3^3)
	2	20 (1)	15 (1)
	3*	838 (42)	$2.0x10^3$ (152)
	4*	$7.2x10^5$ ($4.5x10^4$)	$8.4x10^5$ ($5.2x10^4$)
	5*	$5.4x10^5$ ($6.9x10^4$)	$1.9x10^5$ ($1.7x10^4$)
	6*	$4.7x10^5$ ($4.1x10^4$)	$7.7x10^5$ ($6.2x10^4$)
	7*	5.7^4 ($4.2x10^3$)	6.6^4 ($5.0x10^3$)
Theta	1*	$7.3x10^4$ (3.8^3)	$8.3x10^4$ ($4.3x10^3$)
	2	74 (9)	81 (18)
	3	$9.1x10^4$ ($1.5x10^4$)	$9.7x10^4$ ($1.7x10^4$)
	4*	$9.6x10^5$ ($5.3x10^4$)	$1.0x10^6$ ($6.1x10^4$)
	5*	$7.6x10^5$ ($9.4x10^4$)	$5.2x10^6$ ($2.0x10^4$)
	6*	$7.1x10^5$ ($5.4x10^4$)	$9.2x10^5$ ($7.4x10^4$)
	7	$1.9x10^{10}$ ($1.8x10^4$)	$2.2x10^5$ ($2.3x10^3$)

As seen in Tables 3.4 and 3.5, location-based analysis of EEG signals yielded more sensitivity for both device systems between Alpha and Theta frequency powers during low and high levels of cognitive loads.

100 % of electrode channels of both the Emotiv and Compumedics systems were sensitive to the change in Alpha and Theta frequency band powers between different levels of cognitive load.

Table 3.4: Mean of the Alpha and Theta frequency band power of the Emotiv Epoc system data for dual task trials and the single cognitive task trial. Frequency powers calculated per 10 second epoch are averaged per location across trials and the seven participants. Values in parenthesis indicate the standard error. Significant data sets for a two sample t-test ($p<0.05$) are marked with asterisks(*).

Frequency	**Location**	**Low Cognitive Load** Mean Power (SE)	**High Cognitive Load** Mean Power (SE)	**p value**
Alpha	F3*	$7.6x10^4$ ($1.8x10^4$)	1.1^4 ($2.9x10^3$)	$9.3x10^{-5}$
	F4*	$8.0x10^4$ ($1.9x10^4$)	1.2^4 ($3.3x10^3$)	$9.1x10^{-5}$
	C3*	$7.8x10^4$ ($1.9x10^4$)	1.2^4 ($3.2x10^3$)	$9.4x10^{-5}$
	C4*	$7.1x10^4$ ($1.8x10^4$)	1.6^4 ($2.7x10^3$)	$9.3x10^{-5}$
	P3*	$6.9x10^4$ ($1.7x10^4$)	1.0^4 ($2.7x10^3$)	$9.3x10^{-5}$
	P4*	$6.6x10^4$ ($1.6x10^4$)	9.0^3 ($2.4x10^3$)	$9.5x10^{-5}$
Theta	F3*	$1.8x10^4$ ($4.6x10^4$)	6.6^4 ($1.8x10^4$)	$1.8x10^{-4}$
	F4*	$1.9x10^5$ ($4.8x10^4$)	7.4^4 ($2.0x10^4$)	$1.8x10^{-4}$
	C3*	$1.9x10^5$ ($4.7x10^4$)	7.1^4 ($1.9x10^4$)	$1.9x10^{-4}$
	C4*	$1.7x10^5$ ($4.2x10^4$)	5.9^4 ($1.6x10^4$)	$1.7x10^{-4}$
	P3*	$1.6x10^5$ ($4.0x10^4$)	6.1^4 ($1.6x10^4$)	$1.9x10^{-4}$
	P4*	$1.5x10^5$ ($3.8x10^4$)	4.9^4 ($1.4x10^4$)	$1.7x10^{-4}$

Table 3.5: Mean of the Alpha and Theta frequency band power of the Compumedics system data for dual task trials and the single cognitive task trial. Frequency powers calculated per 10 second epoch are averaged per location across trials and the seven participants. Values in parenthesis indicate the standard error. Significant data sets for a two sample t-test ($p<0.05$) are marked with asterisks(*).

Frequency	**Location**	**Low Cognitive Load** Mean Power (SE)	**High Cognitive Load** Mean Power (SE)	**p value**
Alpha	F3*	-30.5 (13.6)	-79.9 (14.1)	$3.1x10^{-7}$
	F4*	-30.6 (3.5)	-47.7 (3.2)	$1.4x10^{-12}$
	C3*	-31.4 (4.7)	-68.3 (6.6)	$4.7x10^{-17}$
	C4*	19.4 (21.4)	-90.3 (26.5)	$8.1x10^{-11}$
	P3*	-151.2 (21.7)	-161.1 (21.8)	0.0027
	P4*	13.4 (3.9)	-8.7 (4.4)	$1.0x10^{-5}$
Theta	F3*	-48.9 (28.5)	-154.5 (29.4)	$5.6x10^{-8}$
	F4*	-47.3 (7.9)	-84.3 (6.6)	$7.4x10^{-10}$
	C3*	-56.2 (9.8)	-130.5 (13.7)	$1.5x10^{-16}$
	C4*	53.0 (44.2)	-171.3 (54.8)	$1.5x10^{-10}$
	P3*	-306.4 (45.0)	-324.2 (45.3)	0.0101
	P4*	37.1 (8.1)	-5.2 (9.2)	$4.4x10^{-15}$

3.2.3 Discussion

The hypothesis that the consumer grade EEG system, the Emotiv Epoc+, would be sensitive to changes in neurological activity associated with changes in cognitive load was investigated in Experiment 2 as described in Methods. The second experiment evaluated the Emotiv Epoc+ in comparison to the research grade Compumedics SynAmps 2/RT Quik-Cap Ag/AgCl 64 channel cap system using single and dual task protocols described in Methods. The single task trial was used as a baseline such that Emotiv Epoc+ and Compumedics system trials could be more accurately compared to better account for prior exposure to the cognitive tasks. Changes in power of the Alpha and Theta frequency band of EEG signals measured by each device were analyzed using paired t-tests. The Emotiv Epoc+ system yielded less sensitivity relative to the Compumedics system as demonstrated in Tables 3.2 and 3.3 through less frequency of significant changes in Alpha and Theta frequency band power. The relative lack of sensitivity is supported by a smaller absolute difference between the dual task trials and the baseline, as well as a generally higher standard error. However in the analysis of significant changes in Alpha and Theta frequency band powers specific to location, both systems yielded 100 % sensitivity to cognitive load changes. The increase in sensitivity gained through location-based analysis is compatible with fMRI studies that show there exist specific neuroanatomical regions that are involved in changes in cognitive load [52]. It is important to note we did not verify distribution of Alpha frequency powers in the data used in the t-test. Verification of a normal data distribution should be performed to support the results of the t-test. That all electrode locations measured significant changes in Alpha and Theta frequency signals may be due to the lack of spatial resolution of EEG signals. Relative to the Compumedics system, the Emotiv Epoc+ experienced a greater increase in sensitivity through location based analysis. It is suspected that the Emotiv Epoc+ electrodes are more variant in their measurement of EEG signals than the Compumedics due to the design of the Emotiv Epoc+ headset. The Compumedics system interfaces with human biosignals through a tightly fitting EEG cap and electrodes with precisely measured impedance values [53]. On the other hand, the fit of the Emotiv Epoc+ is such that

different electrodes would have a different pressure against the head of the user, the impedance which was also not precisely measured and is indicated in colours the levels of: no signal (black), high impedance (red), medium impedance (yellow), and low impedance (green). Location based analysis of EEG signals seemed to mitigate any issue with variance in individual signal measurements.

One limitation of this study was the restriction to the use of the stationary bike as a motor task. As the Compumedics system requires a wired connection to an amplifier and computer, range of motion of the participants was limited and were unable to perform treadmill walking. Considering the limited vertical motion during stationary biking, it is unlikely these results can be directly translated to gait. The focus of subsequent experimental investigations will examine walking.

The Emotiv Epoc+ did not yield equivalent sensitivity to cognitive load changes as the research grade Compumedics system. However, during location based EEG signal analysis the Emotiv Epoc+ was able to measure data that produced significant Alpha and Theta frequency band power changes comparable the that of the Compumedics cap and consistent with a trend supported in literature [33]. As results of Experiment 1 found data obtained from the Muse yielded no sensitivity to changes in neural activity associated with changes in cognitive load levels, further research concerning this thesis will centre around the Emotiv Epoc+ system.

Chapter 4

Characterizing Ambulatory Noise of the Emotiv Epoc+

This chapter describes a study examining and characterizing gait-induced motion artifact towards application of the Emotiv Epoc+ in an ambulatory fashion. Experimental evaluation discussed in Chapter 3 found the Emotiv Epoc+ is sensitive to changes in Alpha and Theta frequency band power changes induced during changes in cognitive load. However, the presence of noise associated with motion artifact in measured EEG data during ambulatory conditions remains an on-going concern. A well-documented work reviewing signal quality of EEG techniques during stationary and walking paradigms, Oliveira et al. concluded that barriers in measurement were predominantly due to motion artifact [6]. While there have been attempts to filter or predict motion artifact in EEG signals, no studies have investigated noise associated with the Emotiv Epoc+ system. The goal of this study was to characterize motion artifacts measured by the Epoc+ system under ambulatory (i.e., walking) conditions. A swim cap technique was employed to isolate noise induced through motion by insulating the Epoc+ electrodes from actual EEG signals. It was hypothesized that the motion artifact: 1) is significant in amplitude compared to the physiological EEG signal, measured by signal-to-noise ratio (SNR), and 2) can be predicted from head acceleration and angular velocity during movement.

The contents of Chapter 4 has been presented at H-Workload Models and Applications conference 2017 and is published online [54].

4.1 Methods

4.1.1 Experimental Setup

Seven healthy young adults, ages 18-25, volunteered to participate in our study. All subjects provided informed written consent; the Office of Research Ethics at the University of Waterloo approved this study protocol. Measurements of head size, which influences the fit of Emotiv Epoc+ system, and height, which influences gait, were taken. Due to the application of the swim cap as described below, hair thickness variability between participants will not influence data. Refer to Table 4.1 for physiological characteristics of all the participants. To ensure a typical representation of gait, participants were screened for musculoskeletal injuries and experiencing pain or discomfort during movement. Participants were also free of lacerations, abrasions, and contusions on their head due to the potential discomfort arising from contact with the silicone swim cap. Participants self-reported any condition that would exclude them from the study.

Table 4.1: Participant descriptive characteristics

Participant	**Head Circumference** (cm)	**Nasion - Inion** (cm)	**Height**(cm)
1	60	40	185
2	57	35	170
3	62	40	168
4	59	34	165
5	61	39	173
6	58	36	185
7	56	34	165
mean (SD)	59 (2)	37 (3)	173 (9)

Following the protocol introduced by Kline et al. [47], a silicon swim cap was used to insulate neural signals from the EEG measurement device. To simulate the conductivity of human skin, the silicone swim cap was wrapped with cotton gauze (Surgifix, 5cm width) saturated with conductive gel. Conductivity of the gel

soaked gauze was measured using a digital multimeter, gel application was adjusted to ensure the measured conductivity was within the range of dry human skin (0.001-0.1 MΩ) [47]. The Emotiv Epoc+ system was otherwise set up normally per manufacturer's use instructions [4]. In the absence of actual neural signals, the electrodes recorded only signal artifacts [47]. Head movement is measured through a three dimensional accelerometer located at the back of the Emotiv Epoc+ headset [4].

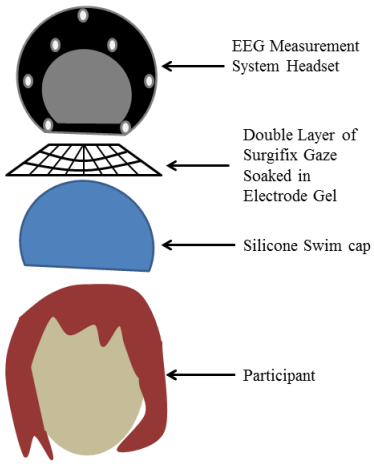

Figure 4.1: Illustration of experimental set up

4.1.2 Data Collection Task

Participants were asked to walk on a treadmill with no incline at set speeds for five minutes. Walking speeds were presented at random order and ranged from very slow to a brisk pace. The four speeds participants walked at were: 1.4 km/h, 2.9 km/h, 4.32 km/h and 5.86 km/h, with each speed is defined as a separate trial during the data collection session. At the start of each trial, prior to initiating the treadmill speed, patients performed three double footed jumps. The purpose of the jumps was to clearly segment each trial, and to synchronize pressure insoles worn by the participant (not used in the current study). After a each walking trial of 5 minutes, the treadmill was stopped and the participant performed another set of five double footed jumps.

4.1.3 Data Processing and Analysis

Collected EEG and head motion data were processed offline using MathWorks' MatLab R2017a [55]. Each trial was segmented into individual trials (4 trials corresponding to the different walking speeds). Using a least squares filter design tool from MatLab, a 4-15 Hz bandpass finite impulse response (FIR) filter was applied to EEG signals (focusing on Alpha and Theta frequencies).

Signal to Noise Ratio

To examine the motion artifact signal amplitude, signal to noise ratio (SNR) was calculated. In the current study, SNR was measured as a ratio of the power of the desired signal (e.g., neural EEG) relative to the power of the noise (e.g., motion artifact), as shown in Equation 4.1.

$$\mathrm{SNR} = 10 * \log_{10}\left(\frac{\sum_{n=1}^{N} X_n^2}{\sum_{n=1}^{N} K_n^2}\right) \quad . \tag{4.1}$$

It is calculated as the ratio of summed squared magnitude of signal, X, to that of the noise, K, measured in decibels.

The isolated noise data collected as described above (i.e., swim cap paradigm) was used to estimate noise levels. Estimates of the neural signal magnitude were calculated from previously collected data reported in Chapter 3 using the Emotiv Epoc+ system from 7 different healthy, young adult participants performing a memory task while sitting stationary (i.e., minimal motion artifact).

Cross-correlation and Detrending

Cross correlation was performed to evaluate which motion signal best represented the energy of the noise data obtained from the electrodes. In performing cross-correlation of each X, Y, and Z axes of the ac-

celerometer and gyroscope signals for each electrode channel, the Z axis accelerometer consistently yielded the highest correlation results. Supported by previous research reporting similar observations [46], Z axis acceleration was used for the rest of data analysis to represent head movement.

Motion induced artifact and head movement data were then detrended to remove offsets introduced through filtering. We employed time and frequency domain system identification techniques to model the introduction of motion artifact into EEG measurements.

Time Domain Analysis

The impulse response function (IRF) provides insight into structure of a system as the time domain representation of a system transfer function [56], [57]. Let $h\,(i)$ represent an IRF such that a linear system is represented by

$$y\ (t) = \Delta t \sum_{t=0}^{T} h\,(i)\,u\,(t-i) \tag{4.2}$$

where *u* and *y* represent the discrete input and output signals, respectively and *t* represents time and *i* represents the independent variable.

The IRF, as defined in Equation 4.2, provides a mathematical representation for analysis of the relationship between movement and noise. In the current study, a correlational approach was used to estimate the IRF through the use of the System Identification Toolbox in MatLab [55].

Time–Frequency Domain Analysis

Due to the periodic nature of the gait cycle, head motion and motion artifact attained during gait are non-stationary signals and simple time and frequency representations may be unlikely to accurately represent the system response [43]. Furthermore, nonlinear relationships may also hinder accurate IRF estimation. To address these limitations, a time-varying wavelet approach was adopted to permit a frequency analysis of the motion artifact.

The wavelet transform provides an advantage over time domain system identification techniques in the ability to model non-linearities [58]. Defined in Equation 4.6, the wavelet transform provides information with respect to a signal $x(t)$ at various time resolutions. This is accomplished by decomposing a signal into various orthogonal wavelets that are derived from a mother wavelet shifted in time and scale [59]. In Equations 4.3 through to 4.8, s represents the scale factor of the wavelet, and τ represents the time location of the wavelet. While there are many different mother wavelet forms, a Morlet Wavelet characterized as a symmetric impulse as many signals and artifacts produced through mechanical dynamics of movement and vibration can be represented by impulses was selected [59], defined in Equation 4.3.

$$\psi_{s,\tau}(t) = \exp(\frac{-\beta^2(t-\tau)^2}{s^2})\cos(\frac{\pi(t-\tau)}{s}) \tag{4.3}$$

$$As\ \beta \to 0\ \ \psi_{s,\tau}(t) \approx \cos(\frac{\pi(t-\tau)}{s}) \tag{4.4}$$

$$As\ \beta \to \infty\ \ \psi_{s,\tau}(t) \approx \delta(x)\ \ . \tag{4.5}$$

where β defines the shape of the wavelet and acts as a balance between resolutions of time and frequency. As β approaches 0, the Morlet Wavelet resembles a cosine function, offering high frequency resolution at the expense of poor time resolution. Conversely as β tends to ∞ the Morlet Wavelet resembles a dirac impulse ($\delta(x)$) function that offers high time resolution at the expense of poor frequency resolution [59].

$$\mathscr{W}\psi, s, \tau = \langle \psi_{s,\tau}(t), x(t) \rangle = |s|^{-\frac{1}{2}} \int x(t)\psi^*_{s,\tau}\rangle dt\ \ . \tag{4.6}$$

To attain a time-frequency representation of the relationship between motion artifact and head acceleration, the magnitude wavelet coherence was calculated. Wavelet coherence is a measure of correlation between two signals and evaluates the degree of coherence and phase relation at each frequency scale. It is defined in Equation 4.9 as the function of power cross spectral density (defined in Equation 4.8) and the power spectral densities (Equation 4.7). The resulting measure, Magnitude Squared Wavelet Coherence, measures

the amount of energy in similar frequencies between two signals at each point in time [58].

$$\mathscr{P}_{\psi,s,\tau}\{x(t)\} = \mathscr{W}_{\psi,\mathbf{s},\tau}\{x(t)\} * \mathscr{W}^{*}_{\psi,\mathbf{s},\tau}\{x(t)\} = |\mathscr{W}_{\psi,\mathbf{s},\tau}\{x(t)\}|^2 \tag{4.7}$$

$$\mathscr{X}_{\psi,s,\tau}\{x(t),y(t)\} = \mathscr{W}^{*}_{\psi,s,\tau}\{x(t)\} * \mathscr{W}_{\psi,s,\tau}\{y(t)\} \tag{4.8}$$

$$\mathscr{C}_{\psi,s,\tau}\{x(t),y(t)\} = | \frac{(|\mathscr{X}_{\psi,s,\tau}\{x(t),y(t)\}|)}{(|\mathscr{P}_{\psi,s,\tau}\{x(t)\}\mathscr{P}_{\psi,s,\tau}\{y(t)\}|)^{\frac{1}{2}}} |^2 \quad . \tag{4.9}$$

4.2 Results

Due to significance in measuring cognitive load and relatively large signal magnitudes, electrode sites AF3 and AF4 will be highlighted in the Results. Positioned over the dorsolateral prefrontal cortex, AF3/4 has been associated (through fMRI and FNIRS studies) with large changes in activity correlated with varying levels of cognitive workload [29]. Furthermore, signals isolating motion artifact acquired in the current study from AF3/4 were large compared to most other sites. Hence, we focus on identification results for these electrodes as a representative cases for all sites.

Initially, data acquired during steady-state walking was processed and analyzed. However, initial results from walking trials yielded poor model fits likely due to lower than expected noise amplitudes. Considering the larger amplitude movement (and noise) associated with the jumps performed at the beginning and end of each walking trial, analysis of the jumps were also conducted and reported.

4.2.1 Walking Trials

Signal to Noise Ratio

By employing the swim cap paradigm, direct measurement of motion artifact levels (i.e., without physiological EEG). As a measure of the potential impact of the motion artifact noise associated with gait, SNR

values indicate a high power of neural signal (measured from participants performing a memory task while stationary, see Signal to Noise Ratio section) relative to motion artifact (i.e., noise). Counter to our hypothesis, high signal magnitudes (8-20 times greater than noise levels) were observed consistently across all locations with the exception of the electrode position O2 (Table 4.2).

Table 4.2: Measured noise magnitude, IRF percentage fit (see Equation 4.10) between the simulated and true system output, and signal to noise ratio (SNR) by electrode site, averaged across all participants at walking speed of 4.32 km/h

Location	**AF3**	**F7**	**F3**	**FC5**	**T7**	**P7**	**O1**	**O2**	**P8**	**T8**	**FC4**	**F4**	**F8**	**AF4**
Noise RMS	24.1	16.9	7.7	6.2	9.0	6.7	6.3	5.6	5.0	6.0	7.2	27.3	4.2	5.3
IRF Percent Fit	9.0	3.6	6.3	7.9	4.1	3.3	1.1	2.1	4.8	5.8	4.3	3.9	5.7	6.1
SNR	20	12	10	13	17	9	11	-1	9	13	8	11	19	14
SNR SD	3	3	2	2	2	2	2	2	2	2	2	2	4	3

Time Domain Analysis

The second hypothesis examined the relationship between head movement and motion artifact. First, a linear approach was generated using the impulse response function (IRF), calculated as in Equation 4.2. Fit of the IRF model was determined by comparing between predicted outputs using the IRF model and the measured outputs of the system (i.e., electrode noise) using Percentage Fit. Equation 4.10 describes the calcuation used where Ym is measured output, Ys is simulated output, and $\overline{Ym}$ is the mean of the measured output.

$$PercentageFit = 100\left(1 - \frac{|Ym - Ys|}{|Ym - \overline{Ym}|}\right) \tag{4.10}$$

An IRF was estimated and evaluated for each electrode site of the Emotiv Epoc+, for every trial of different speed, per participant. Table 4.2 summarizes the noise magnitude and percent fit for each site at 4.3 km/h walking speed. Figure 4.2 allows for a visual comparisons between the measured and simulated signals of site AF3.

In general, the linear IRF models yielded poor representations of the electrode noise measured during the

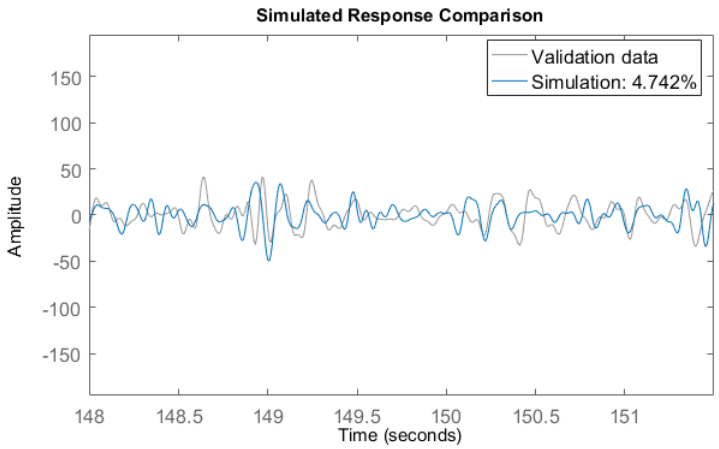

Figure 4.2: Impulse response function (IRF) model simulation of electrode noise alongside measured electrode noise for site AF3 (4.742% fit)

walking trials indicated by low Percent Fit values displayed in Table 4.2. Table 4.3 expands Table 4.2 results of sites AF3 and AF4 across all walking speeds.

Table 4.3: Noise magnitude (RMS) and percent fit between the simulated and measured output averaged across all participants by walking speed for AF3 and AF4

Speed(km/h)	**AF3 Noise RMS**	**AF3 Percent Fit**	**AF4 Noise RMS**	**AF4 Percent Fit**
1.4	8.57	10.2	19.20	5.4
2.9	16.27	9.4	7.95	3.7
4.3	24.14	9.0	5.32	6.1
5.8	21.72	7.2	17.49	5.29

Time-Frequency Domain Analysis

To investigate whether the relationship exhibited time-varying and/or nonlinear characteristics, a wavelet coherence approach was used. Figure 4.3 exhibits the wavelet coherence magnitude, as defined in equations 4.3 to 4.9, between head motion measured during a gait speed of 4.3 km/h, and motion artifact measured at site AF3. The value of 1, denoted in Figure 4.3 by bright yellow, represents the strongest possible wavelet coherence between the two signals, while a value of 0, denoted by deep blue in Figure 4.3, denotes no coherence. A strong coherence indicates similar energy present in the signal occurring at the same frequency

and phase [58]. As shown in Figure 4.3 there exists regions of strong coherence between the head motion and motion artifact signals in the low frequency range of approximately 0.02 Hz to 1 Hz at various periods of time. However, there is little coherence in the frequency bands of interest between 4-15 Hz.

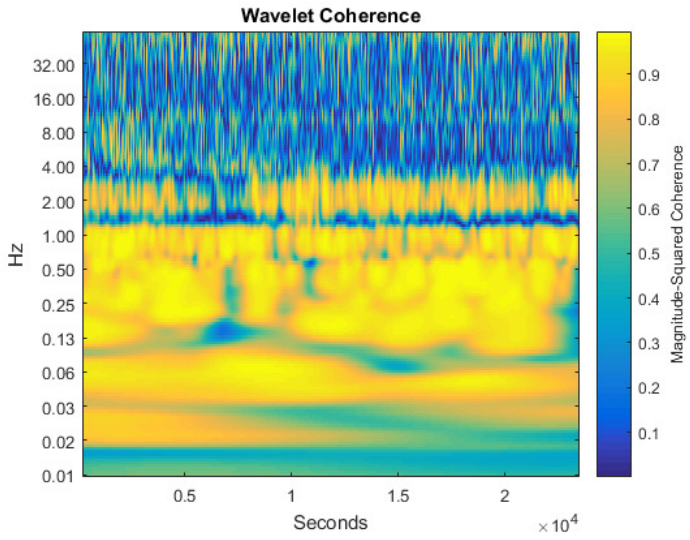

Figure 4.3: Time varying wavelet coherence between motion induced artifact signal and z-axis head movement at a walking speed of 4.3 km/h at AF3

4.2.2 Analysis of Jumps

Periods at which high coherence between head motion and electrode noise were observed in Figure 4.3 to correspond with times of high head motion amplitude. Given this observation, we considered a relationship between head motion and motion artifact only when motion exceeds a threshold (i.e., dead-zone). To test whether this type of nonlinear relationship exists, we chose to specifically examine data recorded during times of known increased head motion. For this, data collected during the jumps participants performed, collected initially for the purpose of segmenting each trial, were examined.

Figure 4.4 plots the wavelet coherence magnitude, during a series of jumps, between head motion and electrode noise measured at electrode position AF3. It can be observed that high amplitude head movement elicits a high coherence with electrode noise in all frequency components in the period of jumps (between

1-2.5 seconds). Table 4.4 shows the Percentage Fit of the electrode noise simulation for every electrode site averaged across all the jumps of all the participants.

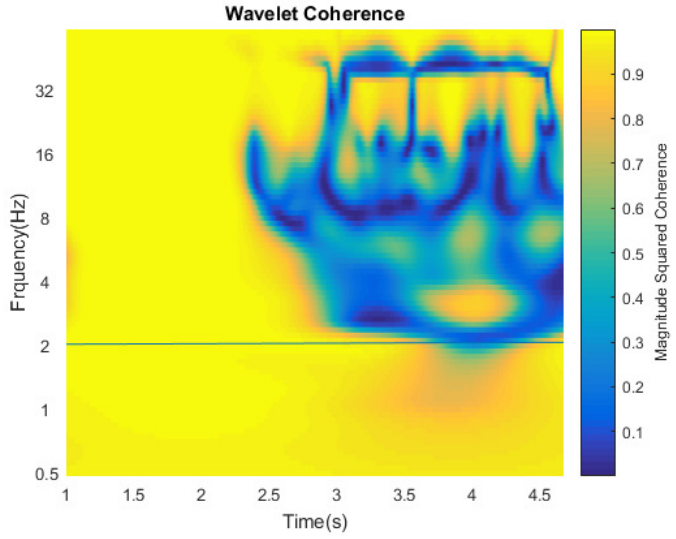

Figure 4.4: Time varying wavelet coherence between AF3 site electrode motion induced artifact signal and z-axis head movement measured during a series of jumps. 5 jumps occurred in the time period between 1 and 2.5 seconds.

Using the jump data, IRFs were used to model and predict electrode noise given the recorded head movement. Figure 4.5 provides a visual comparison between the measured and simulated noise signals of AF3 electrode position. Compared to poor fits from the gait data (10.2% or less), the high amplitude motions yielded significantly more accurate simulations of electrode noise with little variance between electrode sites, as observed in Table 4.4.

Table 4.4: Display of the Percentage Fit (see Equation 4.10) between the simulated and true system output averaged across all participants measured during participants performing jumps

Location	**AF3**	**F7**	**F3**	**FC5**	**T7**	**P7**	**O1**	**O2**	**P8**	**T8**	**FC4**	**F4**	**F8**	**AF4**
Percent Fit	73.6	71.7	71.6	72.2	67.8	70.7	71.3	74.3	71	71.8	71.8	71.8	71.9	72.4

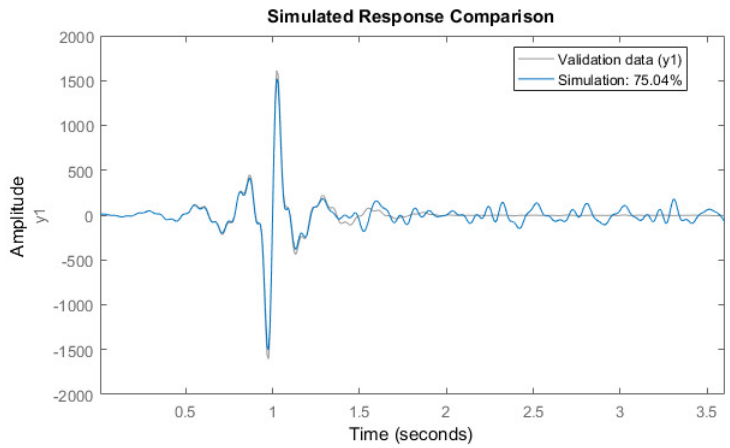

Figure 4.5: Impulse response function (IRF) estimate of electrode noise alongside measured electrode noise for site AF3 during jumps (75.04% fit)

4.3 Discussion

In this study, artifact measured using the Emotiv Epoc+ associated with walking and jumping motions were characterized. Using the protocol described above in Materials and Methods, motion artifact noise was isolated and collected from Emotiv Epoc+ electrodes using a swim cap paradigm. Head motion was measured using a 3D accelerometer built into the Emotiv Epoc+ device [4]. It was hypothesized that motion artifact noise introduced to the EEG signal would: 1) be significant in amplitude compared to the physiological EEG signal, measured by signal-to-noise ratio (SNR), and 2) be predicted from head acceleration and angular velocity during movement.

The data collection protocol used in this study allows for a measurement of EEG signals that are composed solely of system noise isolated from all physiological signals. Using the ground truth noise data of the Emotiv Epoc+ system affords estimates of the SNR attained by the Emotiv Epoc+ in measuring EEG signals at the frequencies relevant for measuring cognitive workload; 4Hz – 15Hz [33]. The SNR estimates show that EEG signals recorded from the Emotiv Epoc+ held 8 to 20 times the power of the noise level (Table 4.2). This high SNR result had the notable location exception of electrode O2, which consistently performed poorly. The cause for the poor signal measurement performance at the electrode location O2 is beyond the

scope of the current study and warrants further investigation.

The high SNR findings from this study support the potential use of the Emotiv Epoc+ system for measuring cognitive workload during ambulatory activities. In particular, the region with the most relevance to measuring cognitive workload is the dorsolateral prefrontal cortex that correspond to electrodes at positions AF3 and AF4 [29]. As shown in Table 4.2, SNR estimates are 20 and 14 for AF3 and AF4, respectively, strongly support the use of these sites to measure cognitive workload.

The second hypothesis of the study anticipated a demonstrable relationship between head movement and motion artifact. Based on signal characteristics, the z-axis of the accelerometer (i.e., vertical plane) was determined as the strongest influence to electrode noise, and was used to model head movement during gait. Impulse response functions (IRF) were estimated to attempt to model the relationship between head movement and motion artifact measured by the Emotiv Epoc+ system during the walking trials, with poor results (no greater than 10.2% fit). The lack of ability to produce a linear model to accurately simulate motion artifact may be attributed to the non-linear nature of the signal.

Using a Time-Frequency analysis, the magnitude square coherence was calculated between electrode noise and head motion. Wavelet transforms are better suited for modelling non-linearities than the IRF method [60]. As such, results of the magnitude squared wavelet coherence, visually depicted in Figure 4.3, provide insight as to how the frequency and time components of noise relate to head movement. While initial results using walking data yielded little coherence in the frequencies of interest, the time-varying wavelet approach permitted a deeper examination of potential factors.

In reviewing data to determine possible causes for coherence varying across time, regions of high coherence corresponded to regions of high amplitude accelerations. This may be attributed to a non-linearity in the relationship between electrode noise and head movement of a dead-zone, indicating that head movement must be at a certain amplitude threshold before it is reflected in electrode noise. To examine this phenomenon further, we analyzed data collected during a known region of high head movement amplitude: as

participants performed jumps. Initially used as a method to segment walking trials, the jump data provided sufficient EEG and accelerometer recording of high amplitude head movement data. Displayed in Figure 4.4 coherence between electrode noise and head movement was greatly increased during the jumps relative to the coherence observed during walking trials. Furthermore the IRF system model was able to simulate electrode noise given head motion data with accuracies ranging between 68% to 74% as shown in Table 4.4. The success in modelling electrode noise using the IRF indicates that, with a certain amplitude of movement, electrode noise is linearly related to head motion. Based on these findings, future research to identify the threshold at which electrode noise linearly relates to head motion is warranted.

In conclusion, it was determined that signals obtained using the Emotiv Epoc+ remain valid to the research of this thesis due to the high SNR results at the electrode locations and frequencies relevant in measuring cognitive workload. Time domain linear system identification of impulse response functions failed to provide an accurate model for simulating motion artifact introduced through head motion during walking. Electrode noise pertaining to regions of high movement amplitude were, however, modelled with a high accuracy using linear system identification. The amplitude of the dead-zone should be must be investigate further to provided insight into the relationship between EEG artifact and movement. In measuring cognitive workload during walking with the Emotiv Epoc+ system, there is confidence that EEG signal noise arising from gait motion will not prove a significant limitation.

Chapter 5

Estimating Cognitive Load using a Commercial EEG system

Building on insights provided in Chapter 3 and 4, the following chapter evaluates the potential of the Emotiv Epoc+ system to distinguish discrete levels of cognitive load during gait in a laboratory setting. The Emotiv Epoc+ system was used to measure EEG signals during treadmill walking in dual task paradigms of varying difficulties with the goal of distinguishing the discrete levels of cognitive load of each paradigm. Data processing techniques explored previously in the thesis, in addition to machine learning classifiers, were applied to EEG data. Based on results obtained in prior chapters it is hypothesized that cognitive load levels can be distinguished from EEG signals measured by the Emotiv Epoc+ under controlled conditions.

5.1 Methods

5.1.1 Experimental Setup

Nine healthy young adults, ages 18-25, participated in this study. All subjects provided informed written consent; the Office of Research Ethics at the University of Waterloo approved this study protocol. Due to

their influence on the fit of the Emotiv Epoc+ and gait, head size and height were measured (displayed in Table 5.1). Height among participants was an average of 170 cm with a standard deviation of 10 cm. Nasion to inion head measurement yielded and average of 35 cm with a standard deviation of 2. Circumference of the head measured above the brow among participants was an average of 57 with a standard deviation of 3. The Emotiv Epoc+ was set up and positioned on the head of each participant according to manufacturer directions (Refer to Appendix A.2) [4].

Table 5.1: Head sizes and height measured from subjects participating in the study.

Study No.	**Head Circumference** (cm)	**Nasion - Inion** (cm)	**Height**(cm)
1	56	34	168
2	57	35	167
3	59	37	182
4	56	34	160
5	62	36	180
6	52	32	157
7	59	36	177
8	54	32	158
9	56	36	178
mean (SD)	57 (3)	35(2)	170(10)

5.1.2 Data Collection Task

During the study, participants performed three cognitive levels of dual task trials. Each trial involved walking on a treadmill at approximately walking speed (2.9 km/h) while performing an auditory n-back test for three minutes. The auditory n-back is a working memory task involving a recording of a random series of integers from one to six, presented to participants using a laptop speaker at 1 Hz. Participants were instructed to say the work 'match' when the current integer matches the integer heard n times ago, where n is the number of integers preceding the current stimulus. For example, for the 1-back test, participants indicated a match when hearing a integer that is the same as the one they just heard. Participants performed 1-, 2-, and 3-back tests to simulate cognitive difficulties of low, medium, and high respectively [51].

5.1.3 Data Processing and Analysis

Data processing was performed offline using MatLab 2017a. Data in the frequencies of interest, Alpha (8-14 Hz) band and Theta(4-7 Hz) band, were first extracted from EEG electrode data using a least squares FIR bandpass filter creating two sets of data. To account for irregularities in the start up and ending of the trials 30 seconds was taken from the beginning and end of each trial. A 10 second Kaiser window then segmented the data, dividing each electrode channel was divided into a set of 10 second data epochs. To account for DC offset, each epoch was detrended using the mean of data across every electrode channel and all time epochs. Frequency band power was calculated per 10 second epoch by the squared of the root mean squared(RMS) value (Equation 3.1). The data processing described was applied to both Alpha and Theta data sets.

Statistic Analysis

Frequency band powers of all nine participants were combined for a group Alpha frequency band power data set, and and a group Theta band power data set. A natural logarithm was applied to shift the data sets into a normal distribution. A separate Analysis of Variance (ANOVA) was conducted for each electrode location and frequency band with cognitive load states (i.e., 1-, 2-, and 3-back) as the main effect. Significant differences are defined by a p value less than or equal to 0.05.

Classification

Towards the goal of identifying levels of cognitive load based on data acquired from the Emotiv Epoc+, a classification algorithm was developed and tested. Using MatLab's Statistics and Machine Learning Toolbox [55], 3 classifier methods were attempted: 1) Decision Tree, 2) Neural Net, and 3) a quadratic kernel Support Vector Machine (SVM) multi-class. Initial results indicated that the SVM generated the highest accuracy and was selected for further development. Briefly, the SVM was defined using a one versus one coding design with binary learners, there exists K(K-1)/2 binary learners for K classes. In the current

scheme, 3 classes are considered. For each binary learner, one class is positive, another is negative, and the rest are ignored. The algorithm exhausts all possible class pair combinations and searches for a hyper-plane for for maximal margin between positive and negative classes [61]. In Equation 5.1, $F(x)$ defines the hyper-plane manipulated through SVM. The goal of SVM is to find a β and b to minimize $||\beta||$ such that $y_j f(x_j) \geq 1$ for all data points (x_j, y_j).

$$F(x) = x'\beta + b \tag{5.1}$$

where x is observations, β represents coefficients of an orthogonal vector to the hyper-plane, and b is the bias term.

Due to class observations of the data set obtained during this study, it was determined a non-linear hyper-plane boundary would most optimally divide classes. The non-linear SVM operates in the transformed predictor space of the Gram Matrix defined by Equation 5.2 as an n by n matrix of elements (j, k) mapped to the linear transformed predictor space by the kernel function ϕ.

$$G(x_j, x_k) =< \phi(x_j), \phi(x_k) > \tag{5.2}$$

The kernel function for a quadratic SVM is further defined in Equation 5.3 [61].

$$G(x_j, x_k) = (1 + x_j' x_k)^2 \tag{5.3}$$

The predicted class is governed by the smallest binary loss, which determines how well the binary learner classified observations to classes using loss weighted decoding [62]. The use of loss weighted decoding, defined below in Equations 5.4, keeps all loss values of various classes in the same range, improving classi-

fication [63].

$$k = argmin_k \frac{\sum_{j=1}^{L} |M_{kj}| g(M_{kj}, s_j)}{\sum_{j=1}^{L} |M_{kj}|} \tag{5.4}$$

where k represents the predicted class for the observation, M_{kj} is the element in matrix M of class k and binary learner j, s_j is the score for the observation of the binary learner j, and $g(...)$ represents a binary loss function. The binary loss function of the quadratic SVM is score between 0 and 1 and is defined in Equation 5.5.

$$\frac{[1 - M_{kj}(2s_j - 1)]^2}{2} \tag{5.5}$$

In the current study, cognitive load associated with the 1-back, 2-back, and 3-back cognitive tasks are considered low, medium, and high, respectively. A matrix was composed of data measured from all participants, where each element of the matrices was a frequency band power averaged over a 10 second epoch. The classifier was trained with 28 features composed of Alpha and Theta frequency bands measured from the 14 electrode locations. The compilation of data across all participants resulted in 73 observations per trial, yielding 219 total observations across all participants and trials. Five fold cross validation was applied to estimate a prediction of accuracy of the final model. Cross validation is a technique used to assess a classification model that is efficient with use of data, ideal for the current small data set. The model assessment technique randomly partitions the original data into five partitions of roughly equal size, four of which are used to trial the classification model, and one data partition (20% of the data) is used to asses model performance. Training and testing are run five times such that each randomly selected partition subset is used once for classifier model assessment. Accuracy yielded by the five fold cross validation is the average of the accuracy across all five train and testing runs.

5.2 Results

5.2.1 Statistic Analysis

The means and standard error of Alpha and Theta powers across participants by cognitive task and electrode channel are displayed in Table 5.2 and Table 5.3, respectively. Using the ANOVA, as defined in Methods, the significance of cognitive level are also displayed in Tables 5.2 and 5.3. The p values calculated through the ANOVA demonstrated significant differences in Alpha frequency band power of different cognitive load levels for the majority of the electrode locations, and some electrode locations for the Theta frequency band power changes. Electrodes AF3, F3, T8 and AF4 showed no significance in the Alpha frequency band power difference between cognitive load levels, and all electrodes except for T7, P8, and FC6 showed no significance in the Theta frequency band power difference.

Table 5.2: Arithmetic mean, and standard error within parentheses, of the Alpha frequency band power per cognitive task and electrode location. Results of the ANOVA of Alpha frequency band powers between cognitive tasks (1-back, 2-back, and 3-back) per electrode location displayed as p values, at a significance of p-value ≤ 0.05. Significant electrode sites are indicated with an asterisk(*)

Location	**Alpha Power**			**p value**
	1–back Mean Power(SE)	2–back Mean Power(SE)	3–back Mean Power(SE)	
AF3	469.4 (90)	243.4 (40)	191.9 (21)	0.35
F7*	588.4 (139)	203.8 (35)	158.6 (19)	0.05
F3	241.9 (65)	150.3 (33)	136.1 (32)	0.14
FC5*	270.1 (71)	75.0 (9)	58.7 (6)	0.006
T7*	470.7 (97)	180.6 (38)	94.0 (10)	0.00002
P7*	135.5 (57)	59.4 (8)	39.9 (3)	0.02
O1*	233.1 (62)	95.0 (10)	78.6 (9)	0.0064
O2*	173.8 (57)	76.8 (8)	60.9 (6)	0.0008
P8*	313.9 (73)	106.5 (11)	85.1 (9)	0.002
T8	403.6 (99)	147.5 (20)	123.3 (17)	0.34
FC6*	261.9 (64)	93.8 (9)	83.2 (8)	0.0003
F4*	248.3 (62)	108.4 (22)	92.8 (17)	0.05
F8*	561.1 (124)	179.2 (25)	142.5 (16)	0.0003
AF4	500.2 (121)	169.2 (24)	181.3 (21)	0.45

Table 5.3: Arithmetic mean, and standard error within parentheses, of the Theta frequency band power per cognitive task and electrode location. Results of the ANOVA of Theta frequency band powers between cognitive tasks (1-back, 2-back, and 3-back) per electrode location displayed as p values, at a significance of p value ≤ 0.05. Significant electrode sites are indicated with an asterisk(*)

Location	**Theta Power**			**p value**
	1–back Mean Power(SE)	2–back Mean Power(SE)	3–back Mean Power(SE)	
AF3	2115.9 (381)	1131.5 (188)	856.1 (75)	0.32
F7	2360.8 (633)	819.6 (181)	627.4 (92)	0.45
F3	581.3 (142)	417.1 (62)	390.4 (66)	0.13
FC5	860.3 (239)	216.4 (25)	170.7 (17)	0.06
T7*	1718.5 (451)	516.4 (176)	303.3 (33)	0.01
P7	267.2 (132)	160.6 (17)	131.3 (11)	0.28
O1	1026.0 (183)	842.4 (177)	807.1 (169)	0.39
O2	424.4 (133)	248.1 (21)	204.2 (18)	0.06
P8*	944.2 (246)	285.2 (30)	241.3 (21)	0.04
T8	1647.5 (448)	413.9 (60)	356.8 (52)	0.30
FC6*	757.3 (188)	266.0 (24)	258.6 (20)	0.05
F4	579.9 (139)	282.7 (42)	322.5 (48)	0.27
F8	2092.3 (564)	615.2 (103)	465.2 (49)	0.09
AF4	2144.8 (553)	977.8 (137)	968.8 (118)	0.80

5.2.2 Classification Results

Initial results examining 3 classifiers yielded 51 %, 60 %, and 68 % accuracy for Decision Tree, Neural Net, and SVM methods, respectively. COnsidering the best result for SVM, this method was selected for further development. Following parameter optimization, the quadratic SVM classifier achieved a 70.3 % accuracy in classification of low, medium, and high cognitive load levels (corresponding to 1-, 2-, and 3-back tasks). The confusion matrix shown in Figure 5.1, tabulating actual and predicted observations, illustrates the performance of classifier in classifying observations of the three cognitive load levels.

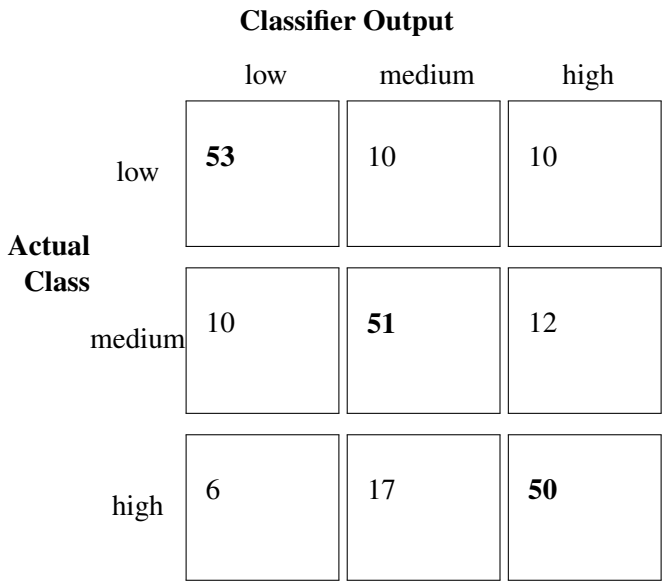

Figure 5.1: Confusion matrix comparing observations for each cognitive load level classified correctly or incorrectly. Correct classifications are on the diagonal in bold.

5.3 Discussion

The objective for this study was to evaluate whether EEG signals measured from the Emotiv Epoc+ can be used to differentiate between dual-task cognitive load levels associated with a standard working memory task. Cognitive load levels were induced through three levels of an auditory n-back task: 1-back inducing low cognitive load, 2-back inducing a medium cognitive load, and 3-back inducing a high cognitive load, while walking on a treadmill at self-selected speed (approximately (2.9 km/h). Two methods were used to distinguish load levels were investigated: 1) a linear statistical method (ANOVA), and 2) a support vector machine (SVM) learning technique.

The ANOVA analysis was used to evaluate whether Alpha and Theta frequency bands powers were sensitive to cognitive load levels at each of the 14 electrode locations. The significant results across the majority of Alpha (10 of 14 locations) powers acquired using the Emotiv Epoc+ indicate a strong difference in cognitive load. The fewer electrode locations that measured significant frequency power changes in the Theta band (3 of 14 locations) may relate to the narrow range of Theta frequency relative to Alpha frequencies. Powers

of both Alpha and Theta frequencies consistently diminished with increasing task difficulty, corroborating a study performed in a stationary paradigm by Antoneko and Niederhauser [36]. Investigating cognitive load with respect to learning environments, a significant decrease in Theta and Alpha oscillatory rhythms was observed in conditions participants associated with a high cognitive load. Similarly, Gerlic and Jausovec confirmed their hypothesis that change in Alpha frequency power can be measured as a determining factor for cognitive load through multi-media learning environments [37]. The diminishing power levels are also a strong indicator that significant findings are unlikely a result of motion artifact.

As both Alpha and Theta frequency bands measured by the Emotiv Epoc+ showed significant changes between different levels of cognitive load, these signals were used as features for the classification of cognitive load levels. While the mean Theta and Alpha frequency powers demonstrated significant differences between three different levels of cognitive load, there was considerable overlap between classes. As a result, a simple threshold method to differentiate levels of cognitive load was unsuitable given the distribution of the data. A Decision Tree Classifier, Neural Net Classifier, and an SVM Classifier were trained yielding classification accuracy results of 51 %, 60 %, and 68 % accuracy respectively. Given the superior results attained through the SVM kernel, this method was evaluated with greater depth. Overall, the SVM classifier was able to classify three levels of cognitive load at an accuracy of 70.3 %. Considering random selection for a 3-class problem is 33%, the short time window of each observation (10 sec), and limited quantity of data available for training (9 participants), the achieved accuracy represents a promising initial result. Furthermore, the reported accuracy using 10 second epochs indicates the ability to classify cognitive load level with a relatively slight delay from real-time. The accuracy yielded by the group-trained classifier across various participants suggests that frequency band power differences can be generalized across a population and calibration between different subjects is unnecessary.

A limitation of this study is a lack of ability to isolate potential mechanisms for EEG power changes associated with increasing cognitive load. While the high signal-to-noise (SNR) results in Chapter 4 suggest that

motion artifact is not a significant portion of the measured signal during gait, other physiological signals (e.g., eye blinks, electromyogram signals of facial muscles) may also be components of the signal measured by the Emotiv Epoc+ [32]. However, our findings indicate the signals recorded by the Emotiv Epoc+ appear to be promising indicators of cognitive load regardless to their components.

Chapter 6

Conclusion

The possibility of falling is a dangerous risk for older individuals, which may result in serious injury, loss of independence, and/or death [9]. Although the physical and psychological consequences of falls are known and well researched, barriers in time and knowledge of clinicians limit effective implementation of fall prevention programs [18]. As high cognitive load is strongly correlated with gait instability, neural monitoring technology (e.g., EEG) may offer insight into an individual's unique risks [2] [33]. Based on previous literature drawn from other applications, Theta (4-7 Hz)and Alpha (8-14 Hz) frequency band powers tend to decrease with higher cognitive load [32]. Combined with consumer grade EEG systems offering greater accessibility due to lowered time and monetary costs, the aim of this thesis was to investigate the capacity of consumer grade EEG devices to monitor cognitive load during ambulatory conditions.

In Chapter 3 of this thesis, the sensitivity of two different commercial EEG headsets to monitor cognitive load, elicited using established working memory and mental arithmetic tasks, was evaluated. Employing the Interaxon Muse headset, Alpha and Theta frequency band powers were insensitive to cognitive load levels, largely attributable to EEG signals overpowered by motion artifact. Although less sensitive than the research-grade Compumedics system, the Emotiv Epoc+ was able to measure a significant difference in Alpha and Theta frequency powers corresponding to different cognitive load levels. Hence, the remaining

investigations of this thesis centred on the Emotiv Epoc+.

In Chapter 4, methods to characterize motion artifacts associated with treadmill walking were examined. Ground truth motion artifact was obtained by attenuating physiological signals with a swim cap, and the Emotiv electrodes recorded only motion artifact. Using the obtained ground truth noise data, SNR estimates yielded strong signal quality results (signal magnitude 8-20x noise amplitudes) in the locations (13 of 14 sites) and frequencies (4-14 Hz) relevant in measuring cognitive workload. In measuring cognitive workload during walking with the Emotiv headset, we are confident EEG signal noise arising from gait motion will not prove a significant limitation.

While SNR levels were strong, deeper investigation was conducted to examine the structure of the motion artifact signal. We hypothesized that motion artifact was related to head movement measured using an inertial measurement unit (IMU, 3-axis accelerometer, 3-axis gyroscope) located in the Emotiv headset. Time and time-frequency domain modelling techniques were applied to model artifact induced in the EEG signals of the Emotiv Epoc+ at the Z axis. The time domain linear system identification approach (i.e., impulse response functions) failed to provide an accurate model for simulating motion artifact introduced through head motion during walking. Given data from the walking trials, the IRF model simulated a prediction of motion artifact at an accuracy of 1.1-9.0 percent fit. Using time-varying wavelet coherence analysis, a potential non-linear response was observed. Electrode noise pertaining to regions of high movement amplitude were, however, modelled with a higher accuracy, between 67.8 percent fit and 74.3 percent fit, using linear system identification. These initial findings suggest a dead-zone nonlinearity in the relationship between head movement and EEG motion artifact.

In Chapter 5, an experiment was designed to evaluate whether signals acquired from the Emotiv Epoc+ can distinguish three levels of cognitive load. Statistic analysis (ANOVA) yielded significantly diminishing changes in Alpha and Theta frequency band power corresponding to increasing cognitively challenging tasks associated with an n-back working memory task. Both the diminishing pattern of Alpha and Theta frequen-

cies, and the high signal to noise ratio calculated previously, strongly indicate frequency power to be a result of physiological signals and not motion artifacts. It cannot, however, be concluded that the physiological signals measured are only composed of EEG signals as the Emotiv Epoc+ may include other signals. For example, increased effort associated with the task challenge may include EMG signals from facial movements (e.g. eye blinks) and/or electro-oculogram (EOG) signals in addition to EEG signals. Regardless of their composition, our findings demonstrate signals recorded by the Emotiv Epoc+ are significantly associated with cognitive load levels for the condition tested.

Towards developing an ambulatory technique to measure cognitive load, a data set of 219 observations across nine participants at three different cognitive load levels was used to train a quadratic SVM classifier. Overall, the classifier was able to differentiate between the three cognitive load levels at an accuracy of 70.3 % (compared to 33% for random selection in a 3-class problem). These promising initial results support the potential for assessing cognitive load in an ambulatory fashion, including fall risk assessment. The short time window (10 seconds) affords a near real-time indicator of cognitive load to associate with specific activities. For at-risk populations, situations stimulating high cognitive loads may be an immediate fall risk when combined with mobility activities. The proposed system may recognize a high-risk scenario to trigger interventions and minimize the risk of falling.

6.1 Limitations and Future Work

Further development of a cognitive load-based fall risk assessment tool will require further investigation to address key limitations of this research. Specifically, deeper understanding of the Emotiv Epoc+ noise, capabilities to measure a wide range of activities, and larger classifier training data sets are identified. First, the hypothesized dead-zone non-linearity relating EEG motion artifact and head movement should be examined to determine thresholds and influencing factors (e.g., headset fit). As a starting point, Chapters 4 & 5 of this thesis examined EEG signals during various walking speeds. However, the wide range of ac-

tivities that occur during daily life (i.e. ascending, descending stairs, transfers) may induce greater motion artifact that has the potential of confounding EEG signals. Further investigation across a wider range of activities may improve generalizability of the proposed ambulatory assessment approach. While the data set used to train the SVM classifier was sufficient for initial investigation, further collection of Alpha and Theta frequency powers during defined cognitive load environments would allow for more robust training of the classification model to improve accuracy. Data analyzed throughout the experimental investigations of this thesis were collected from small samples of young, healthy people; it is unlikely that results obtained from this sample will translate to the target population of older adults. Further investigations must be performed to investigate the influence of aging on EEG signals, in particular Theta and Alpha oscillatory signals in relation to cognitive load. Finally, in an effort to further increase user comfort, the possibility to reduce the number of EEG electrode sites should be examined such that a more low profile device might be developed.

Bibliography

[1] M. Thompson, J. Thompson, and W. Wenqing, "Brodmann areas (BA), 10-20 sites, primary functions." `www.addcentre.com/Pages/professionaltraining.html`. Online; accessed 22-July-2017.

[2] M. Montero-Odasso, J. Verghese, O. Beauchet, and J. Hausdorff, "Gait and cognition: A complementary approach to understanding brain function and the risk of falling," *Progress in Geriatrics*, 2012.

[3] P. De Sanctis, J. S. Butler, B. R. Malcolm, and J. J. Foxe, "Recalibration of inhibitory control systems during walking-related dual-task interference: A mobile Brain-Body imaging (MOBI) study," *NeuroImage*, 2014.

[4] E. Inc, "Emotiv EPOC+." `www.emotiv.com`, 2014. Online; accessed 20-November-2016.

[5] Y. Athavale and S. Krishnan, "Biosignal monitoring using wearables: Observations and opportunities," *Biomedical Signal Processing and Control*, vol. 38, pp. 22–33, Sept. 2017.

[6] A. S. Oliveira, B. R. Schlink, W. D. Hairston, P. Koing, and D. P. Ferris, "Proposing metrics for benchmarking novel EEG technologies towards Real-World measurements human neuroscience," *Froutiers in Human Neuroscience*, vol. 10, May 2016.

[7] "MUSE meditation made easy." `http://choosemuse.com`, Nov. 2016. Online; accessed 22-November-2016.

[8] A. Padron-Monedero, T. Lopez-Cuadrado, I. Galan, E. V. Martinez-Sachez, and P. Martin, "Effect of comorbidities on the association between age and hospital mortality after fall-related hip," *Osteoporosis International*, vol. 28, pp. 1559+, May 2017.

[9] A. Rogers, J. Ewing, K. E. Rogers, R. Kahlil, M. L. Dennis, D. Blackhurst, and M. L. Kaiser, "Elderly ground level fall: A significant impact on both patient and healthcare system," *Journal of the American College of Surgeons*, vol. 223, pp. 208+, Oct. 2016.

[10] W. H. Organization, "WHO global report on falls prevention in older age," tech. rep., World Health Organisation, 2007.

[11] M. S. S. Kamińska, J. Brodowski, and B. Karakiewicz, "Fall risk factors in community-dwelling elderly depending on their physical function, cognitive status and symptoms of depression.," *International journal of environmental research and public health*, vol. 12, pp. 3406–3416, Mar. 2015.

[12] M.-R. Lin, S. L. Wolf, H.-F. Hwang, S.-Y. Gong, and C.-Y. Chen, "A randomized, controlled trial of fall prevention programs and quality of life in older fallers," *Journal of the American Geriatrics Society*, vol. 55, pp. 499–506, Apr. 2007.

[13] J. M. Rimland, I. Abraha, G. Dell'Aquila, A. Cruz-Jentoft, R. Soiza, A. Gudmusson, M. Petrovic, D. O'Mahony, C. Todd, and A. Cherubini, "Effectiveness of Non-Pharmacological interventions to prevent falls in older people: A systematic overview. the SENATOR project ONTOP series," *PLOS ONE*, vol. 11, pp. e0161579+, Aug. 2016.

[14] M. E. Tinetti, C. Gordon, E. Sogolow, P. Lapin, and E. H. Bradley, "Fall-Risk evaluation and management: Challenges in adopting geriatric care practices," *The Gerontologist*, vol. 46, pp. 717–725, Dec. 2006.

[15] S. R. Lord, A. Tiedemann, K. Chapman, B. Munro, S. M. Murray, M. Gerontology, G. R. Ther, and C. Sherrington, "The effect of an individualized fall prevention program on fall risk and falls in older people: A randomized, controlled trial," *Journal of the American Geriatrics Society*, vol. 53, pp. 1296–1304, Aug. 2005.

[16] M. R. C. Hendriks, S. M. A. A. Evers, M. H. C. Bleijlevens, J. C. M. van Haastregt, H. F. J. M. Crebolder, and J. T. van Eijk, "Cost-effectiveness of a multidisciplinary fall prevention program in community-dwelling elderly people: A randomized controlled trial (ISRCTN 64716113)," *International Journal of Technology Assessment in Health Care*, vol. 24, pp. 193–202, Apr. 2008.

[17] S.-F. Chen, S.-F. Huang, L.-T. Lu, M.-C. Wang, J.-Y. Liao, and J.-L. Guo, "Patterns of perspectives on fall-prevention beliefs by community-dwelling older adults: a q method investigation," *BMC Geriatrics*, vol. 16, Aug. 2016.

[18] E. Vlaeyen, J. Stas, G. Leysens, E. Van der Elst, E. Janssens, E. Dejaeger, F. Dobbels, and K. Milisen, "Implementation of fall prevention in residential care facilities: A systematic review of barriers and facilitators," *International Journal of Nursing Studies*, vol. 70, pp. 110–121, May 2017.

[19] N. M. Kosse, K. Brands, J. M. Bauer, T. Hortobagyi, and C. J. Lamoth, "Sensor technologies aiming at fall prevention in institutionalized old adults: a synthesis of current knowledge.," *International journal of medical informatics*, vol. 82, pp. 743–752, Sept. 2013.

[20] J. M. Hausdorff, S. L. Mitchell, R. Firtion, C. K. Peng, M. E. Cudkowicz, J. Y. Wei, and A. L. Golberger, "Altered fractal dynamics of gait: reduced stride-interval correlations with aging and huntington's disease," *Journal of Applied Physiology*, vol. 82, pp. 262+, 1997.

[21] F. B. Horack, "Postural orientation and equilibrium: what do we need to know about neural control of balance to prevent falls?," *Age and Ageing*, vol. 35, no. 2, 2006.

[22] T. Doi, H. Shimada, H. Park, H. Makizako, K. Tsutsumimoto, K. Uemura, S. Nakakubo, R. Hotta, and T. Suzuki, "Cognitive function and falling among older adults with mild cognitive impairment and slow gait," *Geriatrics Gerontology*, 2015.

[23] R. Lin and J. Gage, "The neurological control," *American Academy of Orthotists and Prosthetist*, vol. 2, pp. 1+, 1989.

[24] R. L. Smith-Ray, S. L. Hughes, T. R. Prohaska, D. M. Little, D. A. Jurivich, and D. Hedeker, "Impact of cognitive training on balance and gait in older adults," *Journals of Gerontology*, 2013.

[25] N. Theill, M. Martin, V. Schumacher, S. Bridenbaugh, and R. Kressig, "Simultaneously measuring gait and cognitive performance in cognitively healthy and cognitively impaired older adults: The basel Motor-Cognition Dual-Task paradigm," *Journal compilation the American Geriatrics Society*, 2011.

[26] I. M. Albertsen, M. Ghédira, J.-M. Gracies, and E. Hutin, "Postural stability in young healthy subjects – impact of reduced base of support, visual deprivation, dual tasking," *Journal of Electromyography and Kinesiology*, vol. 33, pp. 27–33, Apr. 2017.

[27] M. B. van Iersel, R. P. C. Kessels, B. R. Bloem, A. L. M. Verbeek, and M. G. M. Olde Rikkert, "Executive functions are associated with gait and balance in Community-Living elderly people," *The Journals of Gerontology Series A: Biological Sciences and Medical Sciences*, vol. 63, pp. 1344–1349, Dec. 2008.

[28] P. Antonenko, F. Paas, R. Grabner, and T. van Gog, "Using electroencephalography to measure cognitive load," *Educational Psychology Review*, vol. 22, pp. 425–438, Apr. 2010.

[29] F. A. Fishburn, M. E. Norr, A. V. Medvedev, and C. J. Vaidya, "Sensitivity of fNIRS to cognitive state and load.," *Frontiers in human neuroscience*, vol. 8, 2014.

[30] K. K. Sreenivasan, C. E. Curtis, and M. DEsposito, "Revisiting the role of persistent neuralactivity during working memory," *Trends in Cognitive Sciences*, vol. 18, pp. 82–89, Feb. 2014.

[31] K. Gramann, "An introduction to mobile brain/body imageing." 2015.

[32] P. Antonenko, F. Paas, R. Grabner, and T. Gog, "Using electroencephalography to measure cognitive load," *Educational Psychology Review*, vol. 22, pp. 425+, Dec. 2010.

[33] P. Antonenko, F. Paas, R. Grabner, and T. van Gog, "Using electroencephalography to measure cognitive load," *Educational Psychology Review*, 2010.

[34] K. Gramann, D. P. Ferris, J. Gwin, and S. Makeig, "Imaging natural cognition in action," *International Journal of Psychophysiology*, 2013.

[35] L. K. McEvoy, M. E. Smith, and A. Gevins, "Test-retest reliability of cognitive EEG," *lCinical Neurophysiology*, 2000.

[36] P. D. Antonenko and D. S. Niederhauser, "The influence of leads on cognitive load and learning in a hypertext environment," *Computers in Human Behavior*, vol. 26, pp. 140–150, Mar. 2010.

[37] I. Gerlic and N. Jausovec, "Multimedia: Differences in cognitive processes observed with EEG," *Educational Technology Research and Development*, vol. 47, pp. 5–14, Sept. 1999.

[38] G. M. Wojcik, P. Wiergala, and A. Gajos, "Evaluation of emotiv EEG neuroheadset," *Bio-Algorithms and Med-Systems*, vol. 11, pp. 211+, 2015.

[39] T. S. Grummett, R. E. Leibbrandt, T. W. Lewis, D. DeLosAngeles, D. M. W. Powers, J. O. Willoughby, K. J. Pope, and S. P. Fitzgibbon, "Measurement of neural signals from inexpensive, wireless and dry EEG systems," *Physiological Measurement*, vol. 36, May 2015.

[40] Y.-P. Lin, Y. Wang, and T.-P. Jung, "Assessing the feasibility of online SSVEP decoding in human walking using a consumer EEG headset," *Journal of NeuroEngineering and Rehabilitation*, 2014.

[41] M. Duvinage, T. Castermans, M. Petieau, T. Hoellinger, G. Cheron, and T. Dutoit, "Performance of the emotiv epoc headset for p300-based applications," *BioMedical Engineering OnLine*, 2013.

[42] S. O'Regan, S. Faul, and W. Marnane, "Automatic detection of EEG artefacts arising from head movements using EEG and gyroscope signals," *Medical Engineering & Physics*, vol. 35, pp. 867–874, July 2013.

[43] M. K. Islam, A. Rastegarnia, and Z. Yang, "Methods for artifact detection and removal from scalp EEG: A review," *Neurophysiologie Clinique/Clinical Neurophysiology*, vol. 46, pp. 287–305, Nov. 2016.

[44] A. S. Oliveira, B. R. Schlink, W. D. Hairston, P. König, and D. P. Ferris, "Induction and separation of motion artifacts in EEG data using a mobile phantom head device," *Journal of Neural Engineering*, vol. 13, pp. 036014+, June 2016.

[45] J. J. Kavanagh, S. Morrison, and R. S. Barrett, "Coordination of head and trunk accelerations during walking," *European Journal of Applied Physiology*, vol. 94, pp. 468–475, July 2005.

[46] E. Hirasaki, S. T. Moore, T. Raphan, and B. Cohen, "Effects of walking velocity on vertical head and body movements during locomotion," vol. 127, no. 2, pp. 117–130, 1999.

[47] J. E. Kline, H. J. Huang, K. L. Snyder, and D. P. Ferris, "Isolating gait-related movement artifacts in electroencephalography during human walking.," *Journal of neural engineering*, vol. 12, Aug. 2015.

[48] R. Brunken, S. Steinbacher, J. Plass, and D. Leutner, "Assessment of cognitive load in multimedia learning using Dual-Task methodology," *Experimental Psychology*, vol. 49, no. 2, pp. 109–119, 2002.

[49] M. Mielke, R. Roberts, R. Savica, R. Cha, D. Druback, T. Christianson, V. Pankratz, Y. Geda, M. Machulda, R. Ivnik, D. Knopman, B. Boeve, W. Rocca, and R. Petersen, "Assessing the temporal relationship between cognition and gait: Slow gait predicts cognitive decline in the mayo clinic study of aging," *Journals of Gerontology*, 2013.

[50] R. Maskeliunas, R. Damasevicius, I. Martisius, and M. Vasiljevas, "Consumer-grade EEG devices: are they usable for control tasks?," *PeerJ*, 2016.

[51] A. T. Newton, V. L. Morgan, B. P. Rogers, and J. C. Gore, "Modulation of steady state functional connectivity in the default mode and working memory networks by cognitive load," *Hum. Brain Mapp.*, vol. 32, pp. 1649–1659, Oct. 2011.

[52] L. Cocchi, A. Zalesky, A. Fornito, and J. B. Mattingley, "Dynamic cooperation and competition between brain systems during cognitive control," *Trends in Cognitive Sciences*, vol. 17, pp. 493–501, Oct. 2013.

[53] "Neuroscan - world leader in functional neuro imaging." `http://compumedicsneuroscan.com/`. Online; accessed 21-July-2017.

[54] K. Shea and J. Tung, "System identification of motion artifact: Noise in EEG headsets from locomotion," in *H Workload Models and Applications*, Dublin Institute of Technology, Arrow@DIT, 2017.

[55] MathWorks, "MathWorks - makers of MATLAB and simulink - MATLAB & simulink." `https://www.mathworks.com/`, 2016. Online; accessed 22-December-2016.

[56] I. W. Hunter, R. E. Kearney, and L. A. Jones, "Estimation of the conduction velocity of muscle action potentials using phase and impulse response function techniques," *Medical and Biological Engineering and Computing*, vol. 25, pp. 121–126, Mar. 1987.

[57] D. T. Westwick and R. E. Kearney, "Identification of physiological systems: a robust method for non-parametric impulse response estimation," vol. 35, no. 2, pp. 83–90, 1997.

[58] D. Chinarro, *System Engineering Applied to Fuenmayer Karst Aquifer (San Julian de Banzo, Huesca) and Collins Glacier (King George Island, Antarctica)*. Springer International Publishing, 2014.

[59] J. Lin and L. Qu, "Feature extraction based on morlet wavelet and its application for mechanical fault diagnosis," *Journal of Sound and Vibration*, vol. 234, pp. 135+, Jan. 2000.

[60] J. B. Thomas, "Using the coherence function as a means to improve frequency domain least squares system identification," Master's thesis, Russ College of Engineering and Technology of Ohio University, Mar. 2007.

[61] T. Hastie, R. Tibshirani, and J. Friedman, *The Elements of Statistical Learning*. 233 Spring Street, New York, NY 10013, USA: Springer Science + Business Media, 2 ed., 2009.

[62] E. L. Allwein, R. E. Schapire, and Y. Signer, "Reducing multiclass to binary: A unifying approach for margin classifiers," *Journal of Machine Learning Research*, pp. 113+, 2000.

[63] J. Fürnkranz, "Round robin classification," *Journal of Machine Learning Research*, pp. 721+, 2002.

Appendix A

Device Standard Operating Procedures

The following appendix details the protocol for use of EEG systems used during the research of the presented thesis.

A.1 Muse 2014

The following protocol is written based off the 'general use' information provided by Interaxon, the manufacturer [7]. Command prompts were used to regulate the reception of the EEG signals from the Muse to attain the raw data.

1. Enable Bluetooth on the chosen control device (e.g. laptop)
2. Hold down the power button on the Muse headset for six seconds to enter pairing mode, all five LEDs will begin to flash in unison.
3. On the control device in Bluetooth settings, select Muse to pair to. Note the Muse device name. The device should indicate that the Muse is paired.
4. Open the command prompt of the control device's operating system and enter: **muse-io –Muse-84CD** (case sensitive) if the Muse device name was "Muse-84CD".

5. Place headset on the user such that the electrodes fit rest against the user's forehead and the support of the headband rests behind the ears.

6. Open a new command prompt window and enter: **muse-player -l 5000 -M muse_recording_name.mat**. This command instructs the computer to record information being sent over a specific port and save the data under the name and data type provided.

A.2 Emotiv Epoc+

The following protocol is written based off of a user manual provided by Emotiv [4]. Please note that important maintenance instructions are further provided by Emotiv that should be adhered to to ensure consistent performance of the Emotiv.

1. Hydrate the felt pads of the sensor units using a saline solution.

2. Remove the sensor units from their case and twist them onto the available gold contacts on the Epoc+ headset.

3. Open the software 'Emotiv Xavier Pure', previously downloaded, on a chosen control device (e.g. laptop).

4. Insert the USB dongle into the control device and turn the headset on using a switch in the back of the Epoc+.

5. Slide the Epoc+ headset onto the head of the user, ensuring correct positioning of the sensor units that may need to be adjusted. The rubber reference electrodes should sit against the mastoid behind the ear.

6. The reference electrodes should be held against the head of the user for five seconds to ensure sufficient connectivity.

7. A diagram in the main user interface indicates the impedance of each electrode. Adjust position of the electrodes and move hair out of the way to ensure all electrodes on the diagram indicate low impedance (green). Higher impedance are indicate by the colours yellow, red and black.

8. Commence session recording through the Emotiv Xavier Pure software.

A.3 Compumedics SynAmps 2/RT Quik-Cap Ag/AgCl 64 channel cap

The following is written based off of a user manual provided by Compumedics [53]. Please note that important maintenance instructions are further provided by Compumedics that should be adhered to to ensure consistent performance of the Compumedics system.

1. Add adhesive double sided tape to two electrodes.

2. Pour approximately 125 mL of electroconductive gel into a disposable cup.

3. Fill a syringe with the electroconductive gel and fasten a blunt tip needle to the end of the syringe.

4. Activate Curry, the graphical user interface developed by Compumedics.

5. Place a small portion of Neuroprep gel on a Kimwipe.

6. Gently abrade with the Neuroprep gel the skin of the two mastoids to clean area of dirt, oil, and dead skin.

7. Clear any Neuroprep residue off of the two mastoids using an alcohol wipe.

8. Attached the two prepared electrodes to the cleaned area of the mastoid surface: one electrode to each mastoid.

9. Measure the subject's head between the nasion and inion and between the preaurical points and calculate the halfway point of each of the two measurements to locate the placement of the CZ electrode.

10. lightly mark the skin in the area determined to be the CZ electrode site.

11. Carefully place the CZ electrode on the marked area.

12. Slide the EEG cap over the subject's head while holding the CZ electrode in place.

13. Check to see that the subject's ears are in the designated ear holes.

14. Secure the cap by attaching the Velcro chin strap across the subject's jaw.

15. Re-measure the distance between the nasion and inion, and the preaurical points. Verify the intersection of the midway points of the two measurements lines up with the CZ electrode. Manoeuvre the EEG cap to ensure the CZ placement.

16. Plug the two electrodes on the mastoids to the M1 and M2 electrode links of the EEG cap.

17. Plug the EEG cap into the Compumedics EEG amplifier.

18. There is a diagram in Curry depicting the impedance of each electrode.

19. Slide the blunt tip needle into the electrode and gently swirl it to abrade skin and move hair out of the way.

20. Apply a small quantity of the electrode gel from the syringe until the impedance displayed in Curry is less than 5 MΩ.

21. Commence session recording through Curry.